RAMA The Research Moored Array for African–Asian–Australian Monsoon Analysis and Prediction*

BY M. J. MCPHADEN, G. MEYERS, K. ANDO, Y. MASUMOTO, V. S. N. MURTY, M. RAVICHANDRAN, F. SYAMSUDIN, J. VIALARD, L. YU, AND W. YU

A new moored buoy array in the historically data-sparse Indian Ocean provides measurements to advance monsoon research and forecasting.

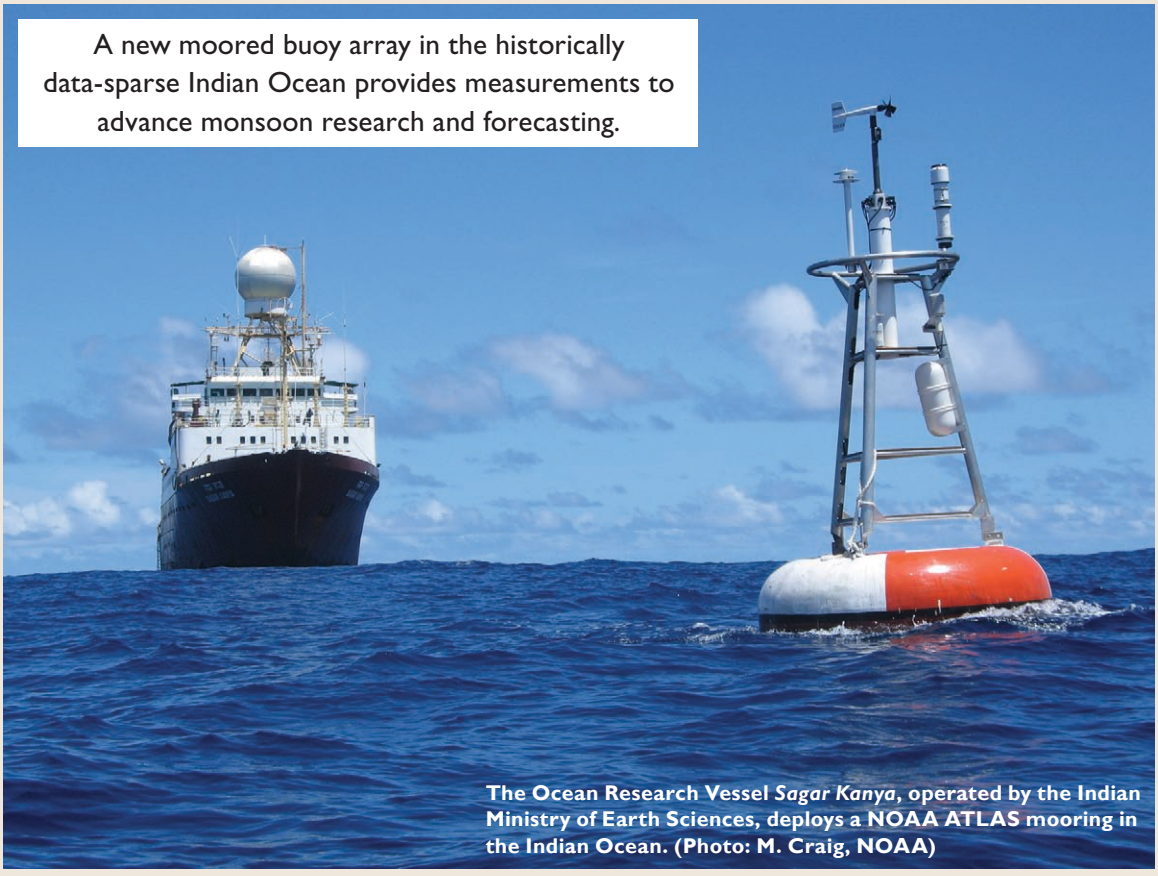

The Ocean Research Vessel *Sagar Kanya*, operated by the Indian Ministry of Earth Sciences, deploys a NOAA ATLAS mooring in the Indian Ocean. (Photo: M. Craig, NOAA)

The Indian Ocean is unique among the three tropical ocean basins in that it is blocked at 25°N by the Asian landmass. Seasonal heating and cooling of the land sets the stage for dramatic monsoon wind reversals and intense seasonal rains over the Indian subcontinent, Southeast Asia, East Africa, and Australia. The Asian landmass also blocks the ocean to the north, so that currents cannot carry heat from the tropics to higher northern latitudes as in the other oceans. Ocean–atmosphere interactions in the region are highly dynamic, involving seasonal current reversals associated with monsoon wind forcing and significant exchanges of heat across the air–sea interface. The Indian Ocean also receives heat from the Pacific via the Indonesian Throughflow (Gordon 2001) while exporting heat to the Atlantic via the Aguhlas Current system (de Ruijter et al. 1999).

Monsoon rains occur each year, supporting agricultural production that provides food for a third of the world's population. These rains are irregular, however, leading to years of drought or flood that have significant socioeconomic consequences (Webster et al. 1999). The failure of Indian summer monsoon rains in 2002 (Waple and Larimore 2003) and excessive rains in equatorial East Africa in late 2006 (Arguez 2007) are recent examples of ▶

*Pacific Marine Environmental Laboratory Publication Number 3199 and National Institute of Oceanography Contribution Number 4437

major disasters. Atmospheric teleconnections carry the effects of Indian Ocean climate anomalies to other regions of the globe, where they affect the evolution of El Niño–Southern Oscillation (ENSO; McPhaden 1999; Zhang 2005), the North Atlantic Oscillation (Hoerling et al. 2001), Sahel rainfall (Giannini et al. 2003), hurricane activity (Maloney and Hartmann 2000), the atmospheric circulation of the North Pacific (Annamalai et al. 2007), and western U.S. weather (Higgins and Mo 1997). Thus, the potential benefits of improved description, understanding, and prediction of the coupled ocean–atmosphere system in the Indian Ocean are enormous. However, the present lack of comprehensive data records for the Indian Ocean severely limits our knowledge of key physical processes and our ability to provide reliable monsoon forecasts even one season ahead.

Observational efforts in the Indian Ocean date back to the International Indian Ocean Expedition of the 1960s (Knauss 1961; National Research Council 2000), which was the first comprehensive study of Indian Ocean circulation and water mass properties. In the 1970s, the Indian Ocean Experiment (INDEX; Luyten and Roemmich 1982) and the Summer Monsoon Experiment (MONEX; Krishnamurti 1985) were designed to improve the description and understanding of seasonally varying oceanic and atmospheric circulations, respectively. The 10-yr (1985–94) Tropical Ocean Global Atmosphere (TOGA) program (National Research Council 1996) and the World Ocean Circulation Experiment (Siedler et al. 2001) with a field phase from 1990 to 1998 were major international efforts to study ocean–atmosphere interactions and basin-scale ocean circulation patterns related to climate. Short-term, regional studies such as the Bay of Bengal Monsoon Experiment (Bhat et al. 2001), the Arabian Sea Monsoon Experiment (Sanjeeva Rao and Sikka 2005), and the Joint Air–Sea Monsoon Experiment (Webster et al. 2002) complemented these broad-scale programs by examining key physical processes controlling variability in specific areas of the Indian Ocean. In contrast to those studies that focused on physical oceanography, ocean–atmosphere interactions, and climate variability, the Joint Global Ocean Flux Study Arabian Sea Expedition (Smith 2001) of the mid-1990s emphasized ocean biogeochemical cycles and biological productivity in relation to monsoon forcing.

These programs laid a foundation for understanding oceanic and atmospheric variability related to the monsoons, but they did not leave a significant legacy of sustained ocean observations in the region (McPhaden et al. 1998). Development of a tropical Indian Ocean observing system progressed very slowly in part because Indian Ocean sea surface temperature (SST) anomalies on interannual time scales were most often within the range of observational errors (e.g., Annamalai and Murtugudde 2004), because there was debate about whether ocean dynamics played a major role in their predictability and because "the predictive relationship between Indian Ocean SST and monsoon rainfall have remained especially poorly characterized . . ." (Clark et al. 2000). By contrast, during TOGA and continuing through the late 1990s as part of the follow-on Climate Variability and Predictability (CLIVAR) program, efforts in tropical ocean observing system development were focused heavily on the Pacific and Atlantic, where ocean–atmosphere interactions were better understood and seasonal prediction efforts were more advanced. The remoteness of the Indian Ocean from first-world countries of North America, Europe, and Asia was also a factor in the relatively slow development of an Indian Ocean observing system compared to the Pacific and Atlantic Oceans.

The past 10 years have seen a rebirth of interest in the Indian Ocean, stimulated by the prominence of the 1997 Indian Ocean dipole (IOD[1]) event (Saji et al. 1999;

[1] The Indian Ocean dipole is also sometimes referred to as the Indian Ocean dipole/zonal mode, or IODZM.

AFFILIATIONS: McPhaden—NOAA/Pacific Marine Environmental Laboratory, Seattle, Washington; Meyers—University of Tasmania, Hobart, Tasmania, Australia; Ando—Japan Agency for Marine Earth Science and Technology, Yokosuka, Japan; Masumoto—University of Tokyo, Tokyo, Japan; Murty—National Institute of Oceanography, Regional Center, Visakhapatnam, India; Ravichandran—Indian National Center for Ocean Information Services, Hyderabad, India; Syamsudin—Agency for the Assessment and Application of Technology (BPPT), Jakarta, Indonesia; Vialard—Laboratoire d'Océanographie et du Climat: Expérimentation et Approches Numériques, IRD, Paris, France; Yu—Woods Hole Oceanographic Institution, Woods Hole, Massachusetts; Yu—First Institute of Oceanography, Qingdao, China

A supplement to this article is available online (10.1175/2008BAMS2608.2)
CORRESPONDING AUTHOR: Dr. Michael J. McPhaden, Pacific Marine Environmental Laboratory, 7600 Sandpoint Way NE, Building 3, Seattle, WA 98115-6349
E-mail: Michael.J.Mcphaden@noaa.gov

The abstract for this article can be found in this issue, following the table of contents.
DOI:10.1175/2008BAMS2608.1

In final form 7 October 2008

Webster et al. 1999; Murtugudde et al. 2000). This event highlighted the dramatic nature and climatic consequences of ocean–atmosphere interactions in the Indian Ocean. The event also drew attention to the relative dearth of measurements in the Indian Ocean and to the opportunities to develop a systematic and sustained ocean observing system there.

This paper describes the rationale for and design of a sustained basin-scale moored buoy array, referred to as the Research Moored Array for African–Asian–Australian Monsoon Analysis and Prediction (RAMA[2]). The array complements other elements of the recently designed Indian Ocean Observing System (IndOOS), which collectively represents an Indian Ocean contribution to the Global Ocean Observing System (GOOS; CLIVAR–GOOS Indian Ocean Panel et al. 2006; Meyers and Boscolo 2006). IndOOS in general, and RAMA in particular, address the need to establish a system for comprehensive, long-term, high-quality, real-time measurements in the Indian Ocean suitable for climate research and forecasting. The broad range of time scales and rapid changes that can occur in the Indian Ocean dictate the need for a moored buoy array providing time series data with high temporal resolution as an essential element of IndOOS. In this respect, RAMA is the Indian Ocean equivalent of the Tropical Atmosphere Ocean/Triangle Trans-Ocean Buoy Network (TAO/TRITON; McPhaden et al. 1998; Kuroda and Amitani 2000) and the Prediction and Research Moored Array in the Tropical Atlantic (PIRATA; Bourlès et al. 2008), which anchor basin-scale observing systems in the tropical Pacific and Atlantic Oceans, respectively, RAMA is targeted at understanding and predicting the East African, Asian, and Australian monsoons, but it will benefit nations outside the Indian Ocean region because of atmospheric teleconnections that influence the far field. In addition, real-time RAMA data will contribute to improved weather and marine forecasts, such as those for tropical cyclones and storm surge. Even though the array is in the initial stages of implementation, the data are already finding practical applications (see the "RAMA helps Australian farmers" sidebar).

The remainder of this paper is organized as follows. We first briefly review the range of phenomena that motivate the study of climate variability in the Indian Ocean region. Emphasis is on intraseasonal-to-interannual time scales and the upper-ocean north of 30°S, where RAMA will have its greatest influence. The reader is referred to Schott et al. (2009) for a more complete account of Indian Ocean phenomenology, including western boundary currents, the Indonesian Throughflow, major surface currents, and the cross-equatorial overturning circulation. We then describe IndOOS and the design criteria for RAMA, followed by a progress report on RAMA implementation. Examples of RAMA data are presented to illustrate their value for research applications, after which we conclude with a brief summary and discussion.

INDIAN OCEAN PHENOMENOLOGY.

Hallmark attributes of the Indian Ocean climate system are the dramatic reversals of the surface winds propelled by seasonally varying land–ocean temperature contrasts. Equally dramatic are the seasonally varying wind-driven ocean currents that affect the evolution of SST (Fig. 1; see also Schott and McCreary 2001; Schott et al. 2009). Associated with monsoon wind variations are pronounced seasonal shifts in atmospheric convection and rainfall over East Africa, southern and eastern Asia, and northern Australia. Collectively, these variations are a regional manifestation of seasonal changes in the Hadley and Walker circulations, which extend throughout the global tropics.

In boreal winter, northeast monsoon winds converge with southeast trade winds in the intertropical convergence zone (ITCZ), located between 5° and 12°S. These wind systems drive a surface ocean circulation that features broad, westward-flowing currents on either side of the equator—the Northeast Monsoon Current and the South Equatorial Current—and a southward-flowing Somali Current along the east coast of Africa. Sandwiched between the two westward currents is the eastward-flowing Equatorial Countercurrent, in geostrophic balance with meridional density contrasts in the Seychelles–Chagos thermocline ridge region (Hermes and Reason 2008; Yokoi et al. 2008). This thermocline ridge, formed by a wind stress curl–driven upwelling in the ITCZ, rises to within 20 m of the surface and results in a zonal band of very thin mixed layers. The SST variations here are sensitive to surface heat fluxes and vertical turbulent heat exchanges with the thermocline because of the low-heat capacity of these thin mixed layers (Duvel and Vialard 2007). Seasonal time-scale SST anomalies in this region can, moreover, remotely influence the subsequent development of summer monsoon rainfall along the western Ghats (Vecchi and Harrison 2004; Izumo et al. 2008).

Wind and circulation patterns in boreal summer are radically different from those in boreal winter.

[2] In Hindu mythology, Rama is an ancient king of India and the hero of the epic "Ramayana."

Southwest monsoon winds drive the currents north of the equator to the east and weaken both the countercurrent and the thermocline ridge. Intense wind-driven coastal upwelling during summer off the Horn of Africa leads to cooling and, through the supply of nutrient-rich thermocline water, high biological productivity in the Arabian Sea. This upwelling is fed by a cross-equatorial circulation cell that is unique to the Indian Ocean, with source waters formed in the southeastern Indian Ocean (~20°–30°S) flowing northward at thermocline depth to the Arabian Sea (Schott et al. 2004). SSTs in Bay of Bengal, on the other hand, remain relatively high during summer, stoking the growth of cyclones that often have a devastating influence on surrounding countries. These high SSTs result in part from a strongly salt-stratified upper ocean capped by shallow freshwater mixed layers that trap surface heat fluxes and inhibit mixing with the thermocline (Shenoi et al. 2002). River runoff and open ocean rainfall supply the freshwater to needed to maintain these thin mixed layers.

During the transition seasons between the northeast and southwest monsoons, winds along the equator are westerly. These winds force the eastward-flowing "Wyrtki jets" (Wyrtki 1973) in April–May and October–November of each year. The Wyrtki jets are important in transporting mass from west to east along the equator and play an important role

RAMA HELPS AUSTRALIAN FARMERS

"No summer rain, then enough to sow in April/May on the arable country, but the plains still missed out. This meant feeding sheep all through autumn and a very-low lambing percentage. Then . . ." Susan Carn is recounting the interplay between weather patterns and management of her farm from the past season. She and her husband, Ben, raise sheep in the low-rainfall area of the Flinders Ranges in south Australia. "So looking back . . . I'm really glad I stuck to my guns and told my husband to stop sowing, as things were not adding up for a good season."

Carn is also the science liaison for the BestPrac farming group in the region. She knows a lot about climate and is always on the lookout for new streams of information to support the decisions they must make throughout the year. The IOD affects rainfall in their region, and Susan was using RAMA data provided by the CLIVAR-GOOS Indian Ocean Panel as an indicator of evolving dipole conditions. The panel was happy to hear this report: "Thank you for sending me the TRITON info. Back in July I showed it to my BestPrac group, who all thought it scary but very useful!"

Modern farmers have many sources of information available to them for improving their bottom lines. Climate information is just one of the sources, but farmers and climate researchers are forging new links to exploit that information. The BestPrac Group meets regularly to share experiences that can enhance their farm management skills. An important part of each meeting is to review the latest seasonal forecasts from the Australian Bureau of Meteorology along with climate indices, such as the Southern Oscillation index and the IOD index. Data from sources such as RAMA moorings are also factored into the deliberations. This information helps the farmers to make informed decisions on a range of practices, such as cropping programs, fertilizer and spray applications, and stocking rates (i.e., the number of animals to keep on the property). The group can then better cope with climate-related risks and capitalize on opportunities. Their motto is "Hope is not a plan!"

Fig. SB1. A BestPrac meeting with members immersed in study. The Carns are on the left. (Photo: John Squires.)

Fig. SB2. BestPrac members fat-scoring sheep to determine if they need supplementary feeding. (Photo: John Squires.)

in the seasonal heat balance of the basin. They are also dynamically linked to variability off of Sumatra and Java through equatorial and coastal waveguide processes (Wijffels and Meyers 2004).

Embedded within the seasonally varying monsoons are energetic intraseasonal oscillations (or ISOs) on weekly to monthly time scales. The best known form of ISO is the Madden–Julian oscillation (MJO), an eastward-propagating wave-like phenomenon in the atmosphere with periods of roughly 30–60 days (Madden and Julian 1994; Zhang 2005). MJO convection is spawned over the Indian Ocean and subsequently propagates eastward as part of a planetary-scale fluctuation in upper-tropospheric winds. Variability in surface winds and deep atmospheric convection is most energetic in regions of warm SST (≥27°C), where interaction with the oceanic mixed layer plays an important role in organizing the MJO (Waliser et al. 1999). Along the equator, intraseasonal wind forcing generates energetic eastward-propagating oceanic Kelvin waves (Han 2005; Fu 2007) which, upon encountering Sumatra, continue poleward as coastally trapped waves. The majority of coastally trapped intraseasonal wave energy propagating southeastward off Sumatra and Java eventually leaks into the Indonesian seas through the Lombok Strait, where it affects throughflow transports (Syamsudin et al. 2004).

The MJO is strongest in boreal winter and spring in the southern tropics, with a secondary peak during boreal summer north of the equator (Zhang 2005). During boreal winter, ocean–atmosphere interactions are particularly strong with large intraseasonal SST variations in the vicinity of the shallow Seychelles–

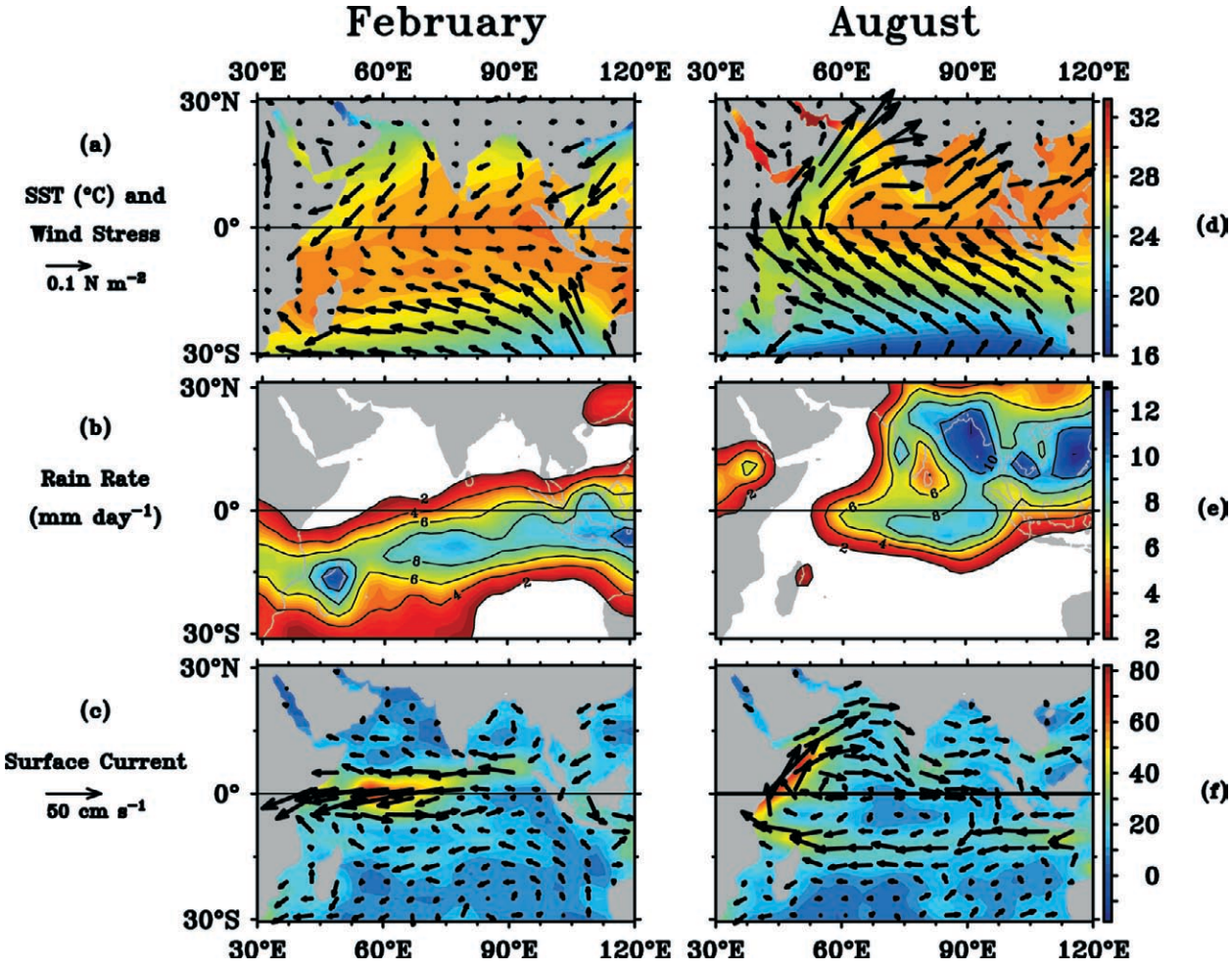

Fig. 1. Monthly means for Feb of (a) surface wind stress and SST; (b) rain rate; and (c) surface current velocity (vectors) and scalar speed (color shading). (d)–(f) Corresponding monthly means for Aug. Rain rate is contoured only for values ≥ 2 mm day^{-1}. SSTs are based on Reynolds et al. (2002); winds are from the 40-yr European Centre for Medium-Range Weather Forecasts (ECMWF) Reanalysis (ERA-40) dataset (http://data.ecmwf.int/data/d/era40_daily/); currents are from Cutler and Swallow (1984); and rain rate is from an analysis of satellite and in situ rain gauge data (Janowiak and Xie 1999).

Chagos thermocline ridge (Duvel and Vialard 2007; Vialard et al. 2008, 2009). In boreal summer, the MJO spins off cloud and rainbands near the equator that propagate poleward over the Bay of Bengal, contributing to alternating "active" periods of enhanced rainfall and "break" periods of reduced rainfall over the Indian subcontinent (Madden and Julian 1994). The number and duration of active/break periods in a particular year determines the net seasonal monsoon rainfall. For this reason, intraseasonal oscillations are often referred to as the "building block of the monsoons."

There are a variety of significant multi-time-scale interactions involving the MJO. For instance, the MJO strongly modulates variability associated with the Wyrtki jets (Han et al. 2004; Masumoto et al. 2005; Sengupta et al. 2007). The diurnal cycle is important in modulating MJO SST variability and ocean feedbacks to the atmosphere (Woolnough et al. 2007). Synoptic time-scale cyclones often develop in association with the MJO (Liebmann et al. 1994; Bessafi and Wheeler 2006; Seiki and Takayabu 2007). Positive IOD events tend to suppress the MJO and higher-frequency atmosphere fluctuations as a result of the reduced convection over the eastern Indian Ocean (Shinoda and Han 2005). Farther afield, propagation of the MJO into the western Pacific affects the evolution of ENSO (McPhaden 1999; McPhaden et al. 2006b; Zhang 2005). The MJO, likewise, influences the development of Atlantic hurricanes (Maloney and Hartmann 2000) and winter storms along the west coast of the United States (Higgins and Mo 1997). There are other notable intraseasonal variations in the Indian Ocean region besides the MJO, such as an oscillation in sea level with a spectral peak at periods near 90 days that Han (2005) attributes to a wind-forced basin-scale oceanic resonance.

The Indian Ocean is characterized by considerable interannual variability, the most prominent mode of which is the response to remote forcing from ENSO (Yamagata et al. 2004; Schott et al. 2009). An eastward shift in the ascending branch of Walker circulation into the central Pacific during El Niño leads to anomalous subsidence, suppressed convection, high-atmospheric surface pressure, and anomalous easterlies over the Indian Ocean. El Niño's influence on precipitation includes reduced Indian summer monsoon rainfall, reduced rainfall in South Africa and Indonesia, and enhanced rainfall in equatorial East Africa. In boreal spring following the peak of El Niño, basin-scale warming occurs as a result of combination of increased surface heat fluxes and, south of the equator, downwelling Rossby waves forced by anomalous ENSO-induced surface wind stresses (Xie et al. 2002; Yu et al. 2005; Schott et al. 2009). The amplitude of this warming is relatively small compared to that in the tropical Pacific, but it leads to increased tropical cyclone activity in the southwest (Xie et al. 2002) and increased rainfall during the following summer over much of the basin (Yang et al. 2007). Oceanic and atmospheric anomalies of opposite sign, which are associated with La Niña events, are also evident in the Indian Ocean region.

Another prominent mode of interannual variability in the Indian Ocean is the IOD. Positive IOD events are characterized by anomalously cold SSTs and suppressed atmospheric convection off Java and Sumatra, warm SSTs and enhanced convection off East Africa, easterly wind anomalies along the equator, and a weak boreal fall season Wyrtki jet (Fig. 2). The IOD is a mode of coupled ocean–atmosphere variability that, like ENSO, develops via feedbacks between zonal wind stress, SST, and thermocline depth anomalies. Unlike ENSO, it is shorter lived and confined mostly to the boreal fall season. Annual mean winds along the equator are westerly in the Indian Ocean, tilting the thermocline down to the east. Thus, it is only during the normal September–November upwelling season off the coast of Java and Sumatra when the thermocline is brought close enough to the surface that ocean–atmosphere feedbacks can take hold. After that, the strong seasonality associated with the onset of the northeast monsoon overwhelms any SST anomalies in this upwelling region that may have developed during the previous summer and fall.

The most recent positive IOD events of significant amplitude occurred in 1994, 1997, and 2006 (Fig. 2e). These events typically lead to above-normal rainfall in East Africa, India, and Southeast Asia, and dry conditions in Indonesia and Australia (Yamagata et al. 2004). Far field impacts of the IOD have also been reported on the seasonal climate of East Asia, Brazil, and Europe (op. cit.). Negative IOD events develop with anomalies and climatic influences roughly opposite to those of positive events.

There is a tendency for positive IOD events to co-occur with El Niño and negative events with La Niña (Meyers et al. 2007). These co-occurrences have complicated the identification of IOD vis-à-vis ENSO climate influences and have raised the question of whether the IOD is fundamentally tied to ENSO (e.g., Chang et al. 2006). However, co-occurrences with ENSO do not account for all IOD events, and the dynamical ocean response to ENSO versus purely IOD wind forcing is not identical (Yu et al. 2005). Thus, while ENSO may be an important triggering

mechanism, the IOD appears to exist as an independent mode of climate variability (Schott et al. 2009).

In addition to interannual variability, the Indian Ocean also experiences longer-term decadal variations and trends. For example, there is a decadal modulation in the frequency of IOD events (Ashok et al. 2004), in the relationship between ENSO and the IOD (Schott et al. 2009), and in the relationship between ENSO and Indian summer monsoon rainfall (Krishna Kumar et al. 1999). Decadal changes in Indian Ocean circulation have been documented, including a decrease in the strength of the Indonesian Throughflow, since 1976 (Wainwright et al. 2008) and an intensification around 2000 of the subtropical cell (Lee and McPhaden 2008), which links upwelling in the Seychelles–Chagos thermocline ridge to source waters formed between 20°–30°S in the southeastern basin. Superimposed on these decadal variations are significant multidecadal warming trends in SST (Cane et al. 1997) and increases in upper-ocean heat content (Levitus et al. 2005) that may plausibly be attributed to anthropogenic greenhouse-gas forcing. The SST trend has been linked to drought in the African Sahel (Giannini et al. 2003) and in the northern hemisphere midlatitudes (Hoerling and Kumar 2003). Latent heat fluxes have increased steadily since

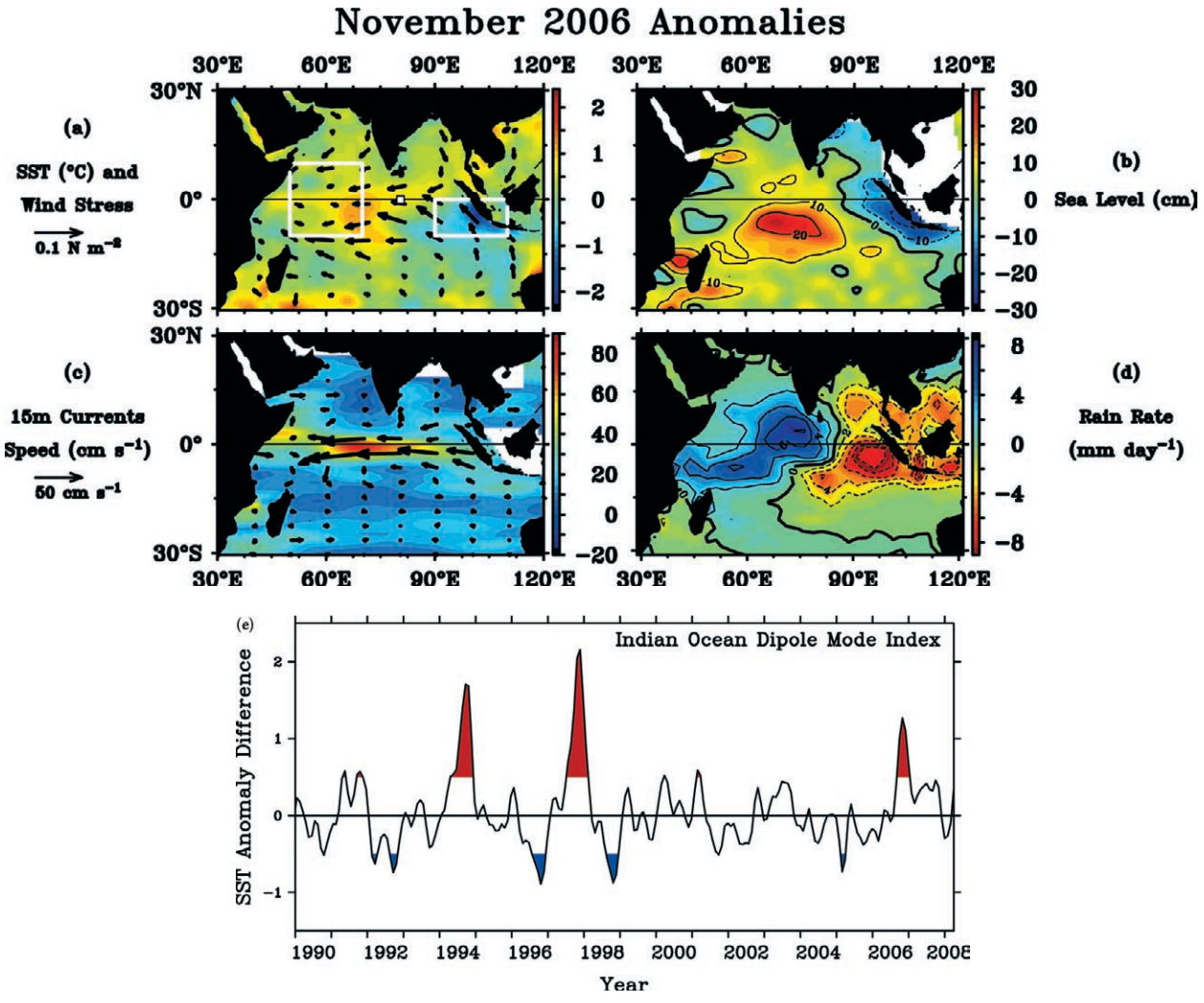

Fig. 2. Monthly anomalies from the mean seasonal cycle in Nov 2006 for (a) SST (based on Reynolds et al. 2002) and Quick Scatterometer (QuikSCAT) wind stress (www.ifremer.fr/cersat/); (b) Jason-1 satellite altimeter sea level anomalies; (c) current velocity (vectors) and speeds (color shading) representative of flow at 15-m depth in the surface mixed layer (Bonjean and Lagerloef 2002); (d) rain rate (Janowiak and Xie 1999). (e) The IOD index for 1990–2008, with the strongest positive (index > 0.5°C) and negative events (index is <−0.5°C) highlighted in red and blue, respectively. The index represents the difference between SST anomalies in the western minus the eastern basin regions outlined in (a). Also shown in (a) is the location of an Autonomous Temperature Line Acquisition System (ATLAS) mooring at 0°, 80.5°E, time series of which are shown in Fig. 8.

the early 1980s over the Indian Ocean (Yu and Weller 2007), suggesting that changes in surface fluxes are a response to, rather than the cause of, this SST trend. It is likely, therefore, that ocean dynamics play a role in producing the observed SST trend, although the precise mechanisms remain uncertain (Alory et al. 2007).

In summary, there is a broad spectrum of phenomena in the Indian Ocean, ranging from diurnal to decadal time scales, that contributes to the observed variability. Quantitative understanding of these phenomena, and how they interact with one another, is undermined though by a sparseness of data. Unlike in the Pacific Ocean where systematic observations as part of the ENSO observing system were initiated in the early 1980s, there are no high-quality multidecadal in situ data records in the upper Indian Ocean, except for those from a few ship-of-opportunity expendable bathythermograph (XBT) lines (Feng et al. 2001; Feng and Meyers 2003). These limitations make it difficult to assess with confidence whether the Indian Ocean–atmosphere system is changing, or may change, as a result of greenhouse gas forcing (Harrison and Carson 2007).

Data limitations also constrain our ability to develop, initialize, and validate coupled ocean–atmosphere forecast models for monsoon prediction. Experimental forecasting with these models is in its infancy, and there are preliminary indications that skillful seasonal forecasts in the Indian Ocean region may be possible at 2–3 season lead times based on ENSO and IOD influences (Luo et al. 2007; Cherchi et al. 2007). Present levels of skill are limited by poor initialization of the subsurface ocean (Wajsowicz 2005), systematic errors in ocean and atmospheric models, and the general inability of either atmospheric general circulation models or coupled ocean–atmosphere models to accurately simulate intraseasonal variability, such as the MJO (Slingo et al. 1996; Zhang 2005). There is evidence to suggest that elements of this intraseasonal variability may be predictable up to 30 days in advance (Webster and Hoyos 2004; Miura et al. 2007), so the fact that this variability is not well represented in dynamical prediction models represents a major challenge in both climate and weather forecasting.

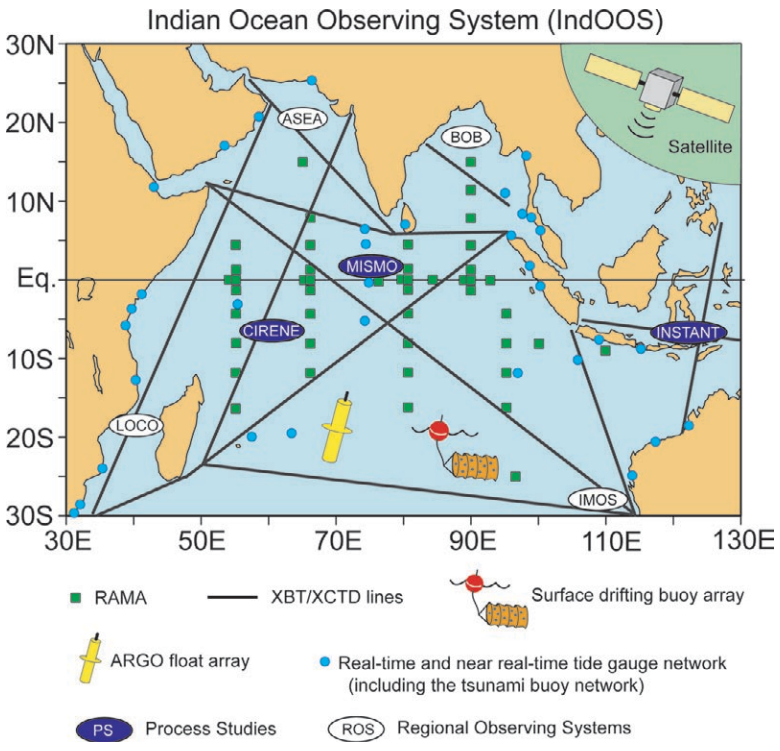

Fig. 3. Schematic of the IndOOS. Green squares indicate the locations of RAMA moorings. Tide gauges are indicated by blue dots. Argo floats and surface drifters are indicated by a single symbol, although many of each are spread throughout the basin (141 drifters and 296 Argo floats as of 31 Aug 2008). XBT and expendable conductivity/temperature/depth (XCTD) sections sampled by ships of opportunity are shown as black lines. Most of these lines are sampled 12–18 times per year at along-track intervals of approximately 1° (though the Australia–Sumatra line and the Australia–Mauritius–South Africa are sampled more frequently to measure details of ocean circulation). Nationally sponsored regional observing systems (ROS) are shown in white ovals: IMOS, LOCO, Arabian Sea (ASEA), and Bay of Bengal (BOB). Process studies (PS) are shown in blue ovals: MISMO, VASCO–Cirene, and INSTANT. The satellite in the upper-right symbolizes the constellation of Earth-observing satellites for SST, surface winds, sea level, and other important oceanic and atmospheric parameters.

RAMA AS A CONTRIBUTION TO INDOOS. *IndOOS*. The international GOOS program and CLIVAR component of the World Climate Research Program (WRCP) established an Indian Ocean Panel (IOP) in 2004 to design and guide the implementation of a basin-scale integrated Indian Ocean observing system for climate research and forecasting. The IOP focused on developing a strategy for in situ mea-

surements to complement existing and planned satellite missions for surface winds, sea level, SST, rainfall, salinity, and ocean color. The resulting system, referred to as IndOOS (Fig. 3), is based on proven technologies, including moorings, Argo floats, ship-of-opportunity measurements, surface drifters, and tide gauge stations (CLIVAR–GOOS Indian Ocean Panel et al. 2006; Meyers and Boscolo 2006). Transmission of data to shore in real time via satellite relay, where feasible, was given high priority to promote the use of the data in climate analysis and forecast products. Network design emphasized the measurement of physical climate variables but recognized that as the science matures and technology advances, widespread inclusion of biogeochemical measurements to support studies of the ocean carbon cycle and ecosystem dynamics would also be possible.

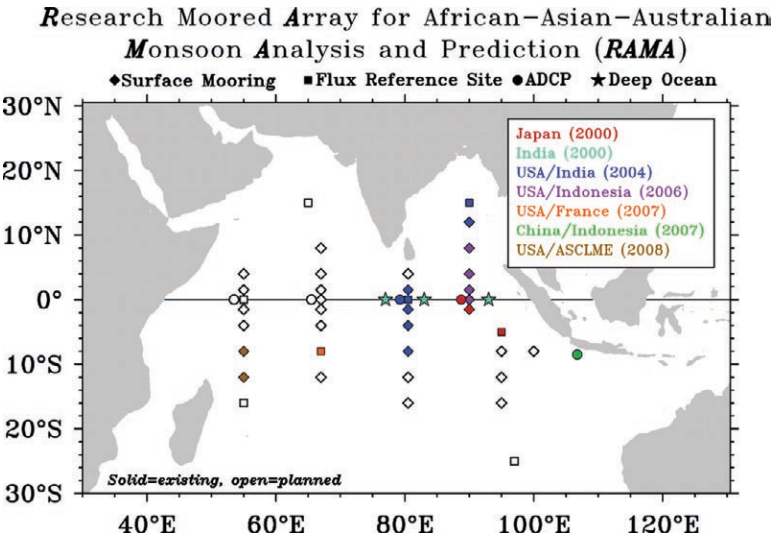

Fig. 4. Schematic of RAMA as of Dec 2008. Filled symbols indicate occupied sites. Color coding indicates national support, with year of first involvement shown in the upper-right box. Open symbols indicate sites not yet instrumented. ASCLME is a consortium of nine African nations including Kenya, Tanzania, Mozambique, South Africa, Madagascar, Mauritius, Seychelles, Somalia, and Comoros.

Embedded in this basin-scale observing system are regionally focused national observing systems. These include Indian efforts in the Bay of Bengal and Arabian Sea, the Australian Integrated Marine Observing System (IMOS; www.imos.org.au), and the long-term ocean climate observations (LOCO; Ridderinkhof and de Ruijter 2003) for western boundary currents in the Mozambique Channel. In addition, IndOOS provides a long-term, broad-scale spatial and temporal context for short-duration, geographically focused process studies, such as the Mirai Indian Ocean cruise for the study of the MJO convection onset (MISMO; Yoneyama et al. 2008), the Validation of the Aeroclipper System under Convective Occurrences (VASCO)–Cirene program (Duvel et al. 2009; Vialard et al. 2009), and the International Nusantara Stratification and Transport (INSTANT) program to study the Indonesian Throughflow (Gordon 2005).

RAMA. A key element of IndOOS is the basin-scale moored buoy array, which we call RAMA (Fig. 4). Some of the Indian Ocean programs described in the beginning collected 1–3-yr-long time series records either near the equator (Knox 1976; Reppin et al. 1999) or in the Arabian Sea (Rudnick et al. 1997). Despite these noteworthy efforts though, there has been no plan until now for a coordinated multinational, basin-scale-sustained mooring array like TAO/TRITON in the Pacific and like PIRATA in the Atlantic.

RAMA addresses the need for such an array. It is designed specifically for studying large-scale ocean–atmosphere interactions, mixed-layer dynamics, and ocean circulation related to the monsoons on intraseasonal to decadal time scales. The planned array consists mainly of 38 surface moorings and 8 subsurface moorings (see the RAMA moorings sidebar). Five of the eight subsurface moorings are acoustic Doppler current profiler (ADCP) moorings to provide long time series measurements of currents in the upper 300–400 m. Four of these ADCP moorings are located along the equator, where geostrophy breaks down and direct current measurements are necessary. A fifth ADCP mooring is also located in the upwelling zone off the coast of Java, where the SST anomalies associated with the IOD first develop. This mooring is near the northern terminus of the frequently repeated Australia-to-Indonesia XBT line (Fig. 3), providing upper-ocean temperature observations at weekly intervals. The primary focus of the array is the upper 500 m, where the ocean and atmosphere most immediately communicate with one another and where intraseasonal-to-decadal time scale variability is most pronounced. However, in addition to the 38 surface and five ADCP moorings, three subsurface moorings along the equator at 77°, 83°, and 93°E are designed to monitor ocean currents down to 4,000 m (Murty et al. 2006).

RAMA MOORINGS

Four types of moorings are presently used in RAMA: surface moorings, surface moorings with enhanced measurement capabilities for comprehensive air–sea fluxes (i.e., "flux reference site" moorings), ADCP moorings, and deep ocean moorings. Each mooring type is described briefly below.

The surface moorings consist of both ATLAS moorings and two different types of TRITON moorings. These moorings have a design lifetime of one year, so they must be serviced annually. Most of the surface moorings are ATLAS moorings supplied by the National Oceanic and Atmospheric Administration's (NOAA's) Pacific Marine Environmental Laboratory (PMEL). These taut-line surface moorings are anchored to the ocean floor in depths of typically 2500–5000 m. Measurements on the surface float include air temperature, relative humidity, wind velocity, downwelling shortwave radiation, and rain rate at heights of 3–4 m MSL. SST and conductivity (which together yield salinity) are measured from the buoy at a nominal depth of 1 m. Sensors on the mooring line measure ocean temperature (12 depths between 10 and 500 m), conductivity (5 depths between 10 and 100 m), mixed-layer velocity (at 10-m depth), and pressure (at 2 depths). A detailed description of the individual sensors, including their heights and depths relative to mean sea level, can be found in the electronic supplement (http://dx.doi.org/10.1175/2008BAMS2608.2). Daily averages of all data and several hourly samples per day of most meteorological variables are transmitted to shore in real time via Service Argos. These data are placed on the GTS for use in operational weather, climate, and ocean forecasting. Higher temporal resolution data (at 1–10-min intervals in most cases) are internally recorded and available after mooring recovery.

Some ATLAS moorings are enhanced with additional instrumentation to more precisely define surface heat, moisture, and momentum fluxes. These flux reference site moorings include sensors for downwelling longwave radiation and barometric pressure. Additional sensors may also be deployed in the upper 140 m of the ocean for finer vertical resolution measurements of temperature, salinity, and velocity. Additional information on ATLAS moorings can be found online (www.pmel.noaa.gov/tao/proj_over/mooring.shtml).

The Japan Marine–Earth Science and Technology Agency (JAMSTEC) has deployed TRITON moorings and, since February 2008, mini-TRITON (m-TRITON) moorings at 1.5°S, 90°E and 5°S, 95°E. TRITON moorings are taut-line moorings designed to be functionally equivalent to ATLAS moorings in terms of sensor payloads, temporal resolution, and data accuracy. There are some differences (e.g., TRITON moorings are deployed with more salinity sensors, and measurements are made to 750 m rather than 500 m), but these differences do not affect comparability of the basic datasets.

After one year of intercomparison with the TRITON mooring at 1.5°S, 90°E, JAMSTEC began to deploy m-TRITON moorings at 1.5°S, 90°E and 5°S, 95°E in February 2008. The m-TRITON sensor and signal processing system are based on those for TRITON, but the mooring system itself is slack line rather than taut line. Slack-line moorings allow for substantial vertical excursions of subsurface sensors as a result of variable currents and winds. Thus, all m-TRITON subsurface sensors are equipped to measure pressure, so that the shape of the mooring line can be determined, after which temperature and salinity data can be interpolated to standard depths.

Hourly averages of all TRITON and m-TRITON data are transmitted to shore in real time via Service Argos and placed on the GTS. Higher-temporal resolution data (at 1–10-min intervals in most cases) are internally recorded and available after mooring recovery. TRITON and m-TRITON sensor specifications, including heights and depths relative to mean sea level, are described in the electronic supplement (http://dx.doi.org/10.1175/2008BAMS2608.2). More information on TRITON and m-TRITON moorings can be found online (www.jamstec.go.jp/jamstec/TRITON/real_time/overview.php/po.php and www.jamstec.go.jp/iorgc/iomics/index.html, respectively).

ADCP moorings are deployed at several locations in the array. The ADCP is positioned with its acoustic beams pointing upward in a subsurface float typically located at depths 300–400 m below the surface. Velocity profiles are measured at hourly intervals with 8-m vertical resolution. Backscatter from the ocean surface interferes with velocity retrievals in the upper 30–40 m of the water column, so subsurface ADCPs do not measure effectively in this depth range. Hence the need for current meters in the mixed layer on surface moorings. ADCP data are available upon mooring recovery. More information on ADCP specifications can be found in the online supplement (http://dx.doi.org/10.1175/2008BAMS2608.2).

Deep ocean moorings maintained by India's National Institute of Oceanography (NIO) have a subsurface float nominally at 100-m depth, below which six mechanical current meters are attached to the mooring line for velocity measurements down to a depth of approximately 4000 m. Beginning in 2003, upward-pointing ADCPs similar to those used by PMEL and JAMSTEC were added to the near-surface float for additional velocity measurements. Data at 1–2 hourly intervals are available from these moorings on recovery. More technical information on these moorings can be found in the electronic supplement (http://dx.doi.org/10.1175/2008BAMS2608.2) and in Murty et al. (2006).

A Web portal with pointers to data from all moorings is found at www.incois.gov.in/Incois/iogoos/home_indoos.jsp. Subsets of the data are available from www.pmel.noaa.gov/tao; www.jamstec.go.jp/jamstec/TRITON/real_time/php/top.php; and www.nio.org/data_info/deep-sea_mooring/oos-deep-sea-currentmeter-moorings.htm.

The array is intended to cover the major centers of ocean–atmosphere interaction in the open ocean away from western boundary current regions and the Indonesian marginal seas. These regions include the Arabian Sea and the Bay of Bengal; the equatorial waveguide, where wind-forced intraseasonal and semiannual current variations are prominent; the eastern and western poles of the IOD; the thermocline ridge between 5° and 12°S, where wind-induced upwelling and Rossby waves affect SST; the southwestern tropical Indian Ocean, where ocean dynamics and air–sea interaction affect cyclone formation (Xie et al. 2002); and the southeastern basin, where source waters of the cross-equatorial and subtropical circulation cells are formed (Schott et al. 2004). Numerical model design studies have assessed the adequacy of the array to achieve its purposes in the context of other observing system components. Alternative sampling strategies have also been evaluated with the conclusion that the proposed array configuration is scientifically sound and cost effective (Vecchi and Harrison 2007; Oke and Schiller 2007).

Surface heat and moisture fluxes are important in determining mixed-layer temperature and salinity variability. However, surface heat and moisture flux climatologies are poorly known in the Indian Ocean (Yu and McCreary 2004; Yaremchuk 2006; Yu et al. 2007) and in several regions, annual means in net surface heat flux from presently available climatologies typically differ by 30–40 W m^{-2} (Fig. 5). Hence, in each of the key regions described above, plans call for at least one specially instrumented surface mooring as a surface flux reference site.

Surface mooring data are telemetered to shore in real time via the Service Argos satellite relay system. Service Argos then places these data on the Global Telecommunications System (GTS) for transmission to operational weather, climate, and ocean forecasting centers. Internally recorded data from all moorings are postprocessed and quality controlled on recovery, after which they are then posted online for public distribution (see the RAMA moorings sidebar). The RAMA data policy is based on the principle of free, open, and timely access to all data from the array.

PROGRESS TOWARD IMPLEMENTATION OF RAMA. At the end of 2008, RAMA was 47% complete, with 22 of the 46 mooring sites occupied (Fig. 4). Nations that have provided mooring equipment, ship time, personnel, and/or logistic support so far include Japan, India, the United States, Indonesia, China, France, and nine African countries that comprise the Agulhas and Somali Current Large Marine Ecosystems (ASCLME) Project. (Contributing organizations and their year of initial involvement

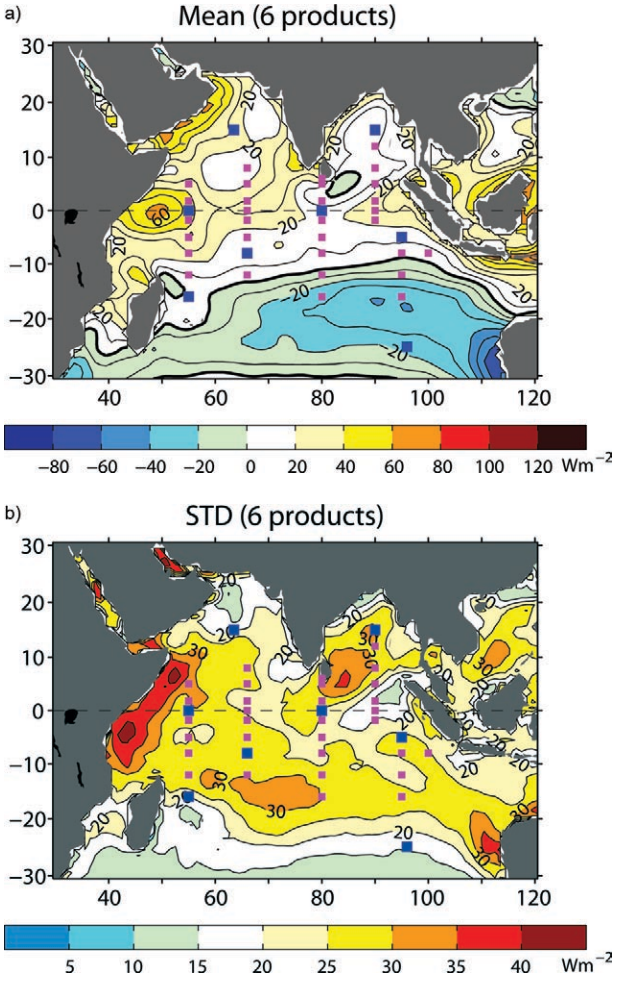

Fig. 5. The (a) average and (b) standard deviation of long-term mean net heat fluxes from six different products. The RAMA array is superimposed on these fields with flux reference sites highlighted as blue squares. The six products are the National Centers for Environmental Prediction–National Center for Atmospheric Research (NCEP–NCAR) Global Reanalysis 1 (NCEP-1) (Kalnay et al. 1996) and NCEP/Department of Energy Global Reanalysis 2 (NCEP-2) (Kanamitsu et al. 2002) fluxes; ECMWF operational fluxes (ECMWF 1994); ECMWF reanalysis fluxes (ERA-40; Uppala et al. 2005); the U.K. National Oceanography Center (NOC) fluxes (Josey et al. 1999); and an OA flux product produced by Woods Hole Oceanographic Institution (Yu and Weller 2007), combined with radiation data from the satellite ISSCP (Zhang et al. 2004). Long-term means for NCEP-1, NCEP-2, OA flux + ISCCP, and ECMWF are based on the period 1983–2004; ERA-40 means 1983–2001; and NOC climatology 1980–2005.

are described in the RAMA implementation time line sidebar.) Given current and projected national resource commitments, the array could be fully implemented by the end of 2012. The CLIVAR–GOOS Indian Ocean Panel and the CLIVAR Tropical Moored Buoy Implementation Panel provide scientific and technical guidance, respectively, for the development of RAMA.

The array will require a reliable, regular supply of ship time to fully implement, since the surface moorings have a design lifetime of one year and must be replaced annually. Making reasonable assumptions about ship speeds, carrying capacity, and ports of call around the Indian Ocean, we estimate that a minimum of approximately 150 days of dedicated ship time per year will be required to maintain the array once complete. For perspective, this requirement is about half that needed to maintain the 70 mooring TAO/TRITON array in the Pacific and about twice that needed to maintain the smaller 18 mooring PIRATA array in the Atlantic. The actual number of sea days required per year to maintain the array may be higher than the absolute minimum, though, since research cruises sponsored by partner countries often address national scientific priorities in addition to those of the RAMA mission.

The greatest impediment to implementation, assuming adequate financial resources and ship time can be found, is vandalism by fishing vessels. Surface buoys are effectively fish aggregation devices (FADs) that attract fish and, consequently, fishermen. Vandalism occurs primarily in pursuit of tuna and affects TAO/TRITON and PIRATA as well as RAMA. Strategies to mitigate vandalism include engineering design improvements to the moorings and outreach to the fishing community. Data losses can also be minimized by scheduling cruises to repair or replace moorings at yearly or more frequent intervals.

DATA AND RESEARCH APPLICATIONS. RAMA, even in the initial stages of development, is providing valuable data for describing and understanding variability in the Indian Ocean. For example, a pronounced semiannual cycle in upper-ocean temperature, salinity, and zonal velocity is evident in the first three years of data from near-equatorial moorings at 90°E (Fig. 6). Hase et al. (2008) relate this variability to remote zonal wind forcing in the central Indian Ocean associated with the monsoon transitions. Upward phase propagation at semiannual periods in both temperature and zonal velocity is presumably the signature of wind-forced equatorial Kelvin waves. This vertical propagation is consistent with, but more sharply defined than, that evident in equatorial time series collected during INDEX in the 1970s (McPhaden 1982; Luyten and Roemmich 1982). The subsurface salinity maximum centered near 100–150 m at 90°E (Fig. 6b) is due to eastward transport along the equator of high-salinity water originating in the Southern Hemisphere subtropics and the Arabian Sea (Taft and Knauss 1967; Schott et al. 2004). Semiannual increases in maxi-

RAMA IMPLEMENTATION TIME LINE

RAMA traces its roots to Indian and Japanese national efforts initiated in 2000. JAMSTEC deployed an ADCP mooring at 0°, 90°E in 2000 (Masumoto et al. 2005) and two TRITON moorings at 1.5°S, 90°E and 5°S, 95°E in 2001 (Hase et al. 2008). NIO also began subsurface mooring deployments to sample the deep ocean along the equator in 2000 (Sengupta et al. 2004; Murty et al. 2006). These efforts, which have continued without interruption, were precursors to RAMA and incorporated into the array design.

Then, in October–November 2004, NOAA/PMEL in collaboration with NIO and the Indian Ministry of Earth Sciences (MoES) deployed four ATLAS moorings and one ADCP mooring near the equator between 80° and 90°E. PMEL and the Indonesian Agency for the Assessment and Application of Technology (BPPT) and the Ministry for Marine Affairs and Fisheries (DKP) occupied sites at 4°N, 90°E and 8°N, 89°E in November 2006. The French-led VASCO–Cirene experiment (Duvel et al. 2009; Vialard et al. 2009) provided an opportunity in January 2007 to establish the flux reference site ATLAS mooring at 8°S, 67°E. In November 2007, a Chinese ADCP mooring was deployed off the coast of Java as part of a collaboration between the Chinese First Institute of Oceanography (FIO), BPPT, and DKP. Also in November 2007, PMEL and Indian technicians deployed two ATLAS moorings in the Bay of Bengal (12° and 15°N, 90°E) on a cruise lead by the Indian National Center for Ocean Information Services (INCOIS). In November 2008, the ASCLME Project, a consortium of nine African countries, joined the RAMA fold by deploying two ATLAS moorings along 55°E (8° and 12°S) from the Norwegian RV *Dr Fridtjof Nansen*.

Efforts to build and sustain the array will continue within a framework of formal bilateral agreements that are either approved or under development between agencies in the various partner countries. In addition, an international "Resource Forum" is being established to coordinate resource commitments across all nations involved in RAMA. Our expectation, based on current and projected resource commitments, is that RAMA will be completed by the end of 2012.

mum salinity values in this subsurface layer are most likely the response to increases in eastward velocity associated with the semiannual Wyrtki jets.

Superimposed on these semiannual variations are energetic 30–50-day period oscillations, which presumably reflect the effects of wind (e.g., Fig. 7a), heat flux, and freshwater forcing on intraseasonal scales. Intraseasonal oscillations are largest for temperature in the thermocline (Fig. 6a) and largest for salinity and zonal velocity in the surface mixed layer (Figs. 6b and 7b). Meridional velocity is most strongly influenced on intraseasonal time scales by 10–20-day period oscillations (Fig. 7c), which are not only evident in the upper 400 m but also at depths greater than 2000 m from the deep ocean moorings along the equator. Sengupta et al. (2004) identified these oscillations as wind-forced mixed Rossby–gravity waves.

Interannual variability associated with the 2006 IOD event was captured by the moored array, as illustrated in the time series from 0°, 80.5°E for two contrasting periods: October–November 2004 and October–November 2006 (Fig. 8). Compared to late 2004, which was near normal in terms of IOD activity (Fig. 2e), zonal surface winds and the zonal mixed layer currents they forced along the equator largely flowed in the opposite direction, that is, to the west, in late 2006 (Figs. 8a,b). The westward

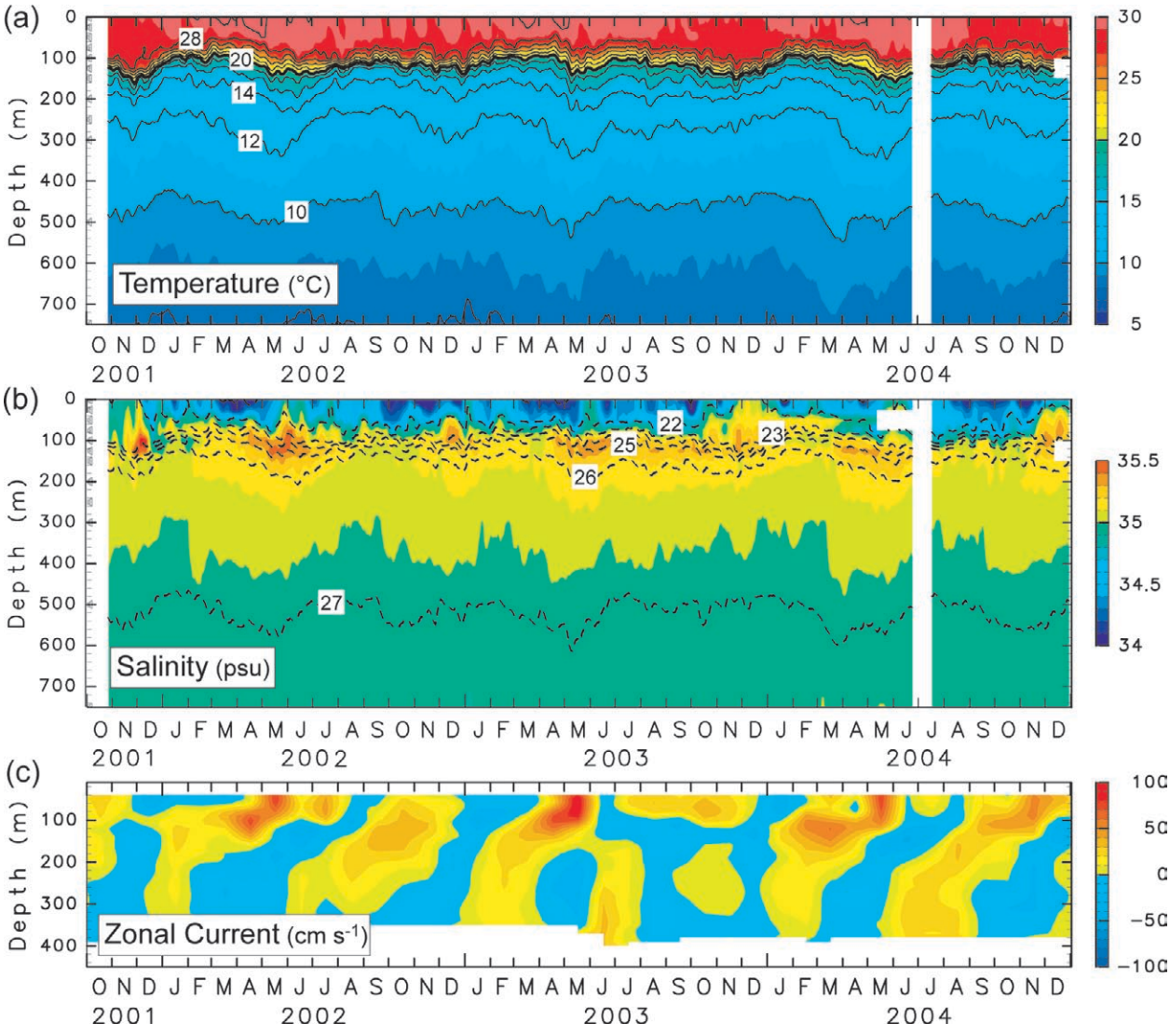

Fig. 6. Time–depth sections of (a) temperature and (b) salinity from 1.5°S, 90°E and (c) zonal velocity from 0°, 90°E. Daily data in (a) and (b) have been smoothed with a 7-day running mean filter and (c) with a monthly filter. Color intervals for the temperature, salinity, and velocity are 1°C, 0.1, and 10 cm s^{-1}, respectively. Thin black lines are at intervals of 2°C for temperature, with 20°C isotherm shown as a thick line. Contours of the potential density at intervals of 1.0 kg m^{-3} are superimposed on salinity sections (based on Hase et al. 2008).

currents drained the eastern basin of upper-ocean mass, which may have contributed to periods of thermocline shoaling at 0°, 80.5°E (Fig. 8c). Also, though SST was only slightly warmer than usual at 0°, 80.5°E (≤1°C) as would be expected for a mooring located outside the IOD SST index regions, these elevated temperatures favored enhanced convection and rainfall in the central basin (Fig. 2). The dramatic drop in mixed-layer salinity of over 1 psu in late 2006 relative to late 2004 at 0°, 80.5°E (Fig. 8d) is consistent with this enhanced rainfall as well as with equatorward flow of low-salinity water from the Andaman Sea (Murty et al. 2008, manuscript submitted to *Ocean. J. Geophys. Res.*). It is also interesting to note that the meridional component of mixed-layer velocity in Fig. 8b exhibits very regular biweekly oscillations, as observed in the 0°, 90°E ADCP data (Fig. 7c) and in the deep ocean moorings along the equator (Sengupta et al. 2004).

Data from the mooring at 8°S, 67°E in the region of the Seychelles–Chagos thermocline ridge illustrate ocean–atmosphere interactions associated with the passage of Tropical Cyclone Dora (Duvel et al. 2009; Vialard et al. 2009). Dora began as a tropical disturbance northeast of the buoy in the vicinity of Diego Garcia (7°S, 72°E) in late January 2007. As this disturbance migrated in a south-southwesterly direction, it intensified to named tropical storm strength on 30 January and to tropical cyclone strength on 1 February. Dora reached a peak intensity of more than 100 kts (51 m s^{-1}) on 3 February, when it was centered near 18°S, 67°E. Afterwards, it continued to track to the southwest, eventually dissipating by 12 February.

Dora passed near the buoy in the early stages of its development (January 25–29), before it became a named tropical storm. Its effects in the real-time daily averaged data can be seen in the sudden change in wind speed and direction, increase in precipitation, decrease in atmospheric pressure, and decrease in incoming shortwave radiation at the buoy site in late January 2007 (Fig. 9, left). Also evident in late January is the abrupt cooling and freshening of the surface mixed layer associated with decreased surface heat fluxes and increased freshwater fluxes. Internally recorded 1–10-min data recovered from the buoy show even greater detail during the last week of January 2007 (Fig. 9, right). We see, for example, a very sharp drop in surface salinity and temperature associated with a nighttime rain event on January 24. Also, SST dropped in a very stepwise fashion by 2°C during the week. Periods of very-low insolation on rainy (and presumably cloudy) days are evident. There is also a pronounced solar semidiurnal tide in atmospheric surface pressure. These data are being analyzed to quantitatively address the relative roles of surface fluxes, vertical turbulent mixing, and horizontal advection in the heat and salt balances for this particular period.

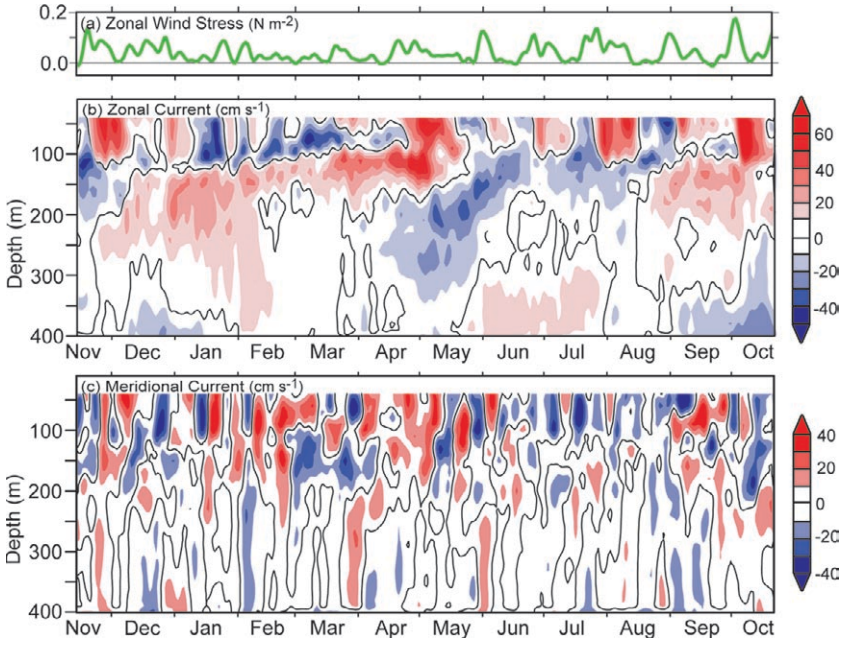

Fig. 7. Time series of (a) zonal wind stress (N m^{-2}) at the sea surface averaged between 80° and 90°E observed by the QuikSCAT satellite. Time–depth sections of (b) zonal current and (c) meridional current observed at 0°, 90°E. The eastward (westward) and northward (southward) currents are shaded in reds (blues), with black contours for zero velocity. Daily data have been low-pass filtered with a 5-day period cutoff (based on Masumoto et al. 2005).

RAMA mooring data can also be used to identify deficiencies in currently available surface flux products as a stimulus to their possible improvement. For example, surface heat fluxes were calculated from data at three of the RAMA mooring sites for comparison with numerical weather prediction (NWP) model flux products, the International Satellite Cloud Climatology Project (ISCCP) radiation product (Zhang et al.

2004) and an objectively analyzed (OA) turbulent heat flux product (OA flux; Yu and Weller 2007). Results (Fig. 10) indicate that ISCCP overestimates solar radiation and underestimates longwave radiation at these sites. The NWP products significantly overestimate latent heat fluxes, such that the net heat flux into the ocean is underestimated by 40–60 W m^{-2} at 0°, 80.5°E. This heat flux deficit, if accumulated in a 50-m-thick mixed layer over three months, would translate into a temperature error of ~2°C, which is equivalent to the seasonal range of SST at this location. The OA flux product slightly underestimates latent heat fluxes at all three locations, but it is a significant improvement on the NWP turbulent fluxes.

SUMMARY AND DISCUSSION. RAMA addresses a long-standing need for a sustained moored buoy array in the Indian Ocean for climate studies. It will take several more years to complete and will require coordinated resource contributions (financial, human, and ship time) from several countries. Implementation of RAMA will result in a globe-girdling network of tropical moored buoy arrays, which includes TAO/TRITON in the Pacific and PIRATA in the Atlantic. Like these other arrays, we can expect that RAMA will fundamentally advance our understanding of large-scale ocean dynamics, ocean–atmosphere interactions, and climate variability in the Indian Ocean region.

We can also expect that RAMA will contribute to operational activities as a component of GOOS, the Global Climate Observing System (GCOS), and the Global Earth Observing System of Systems (GEOSS). Real-time RAMA data available on the GTS are, for example, already being incorporated into weather forecasts and seasonal climate forecasts produced by operational centers. RAMA can likewise provide valuable data for operational ocean state estimation and for oceanic and atmospheric reanalysis products. The array will provide data for validating satellite retrievals and products based on them, such as surface winds, SST, rainfall, and mixed-layer

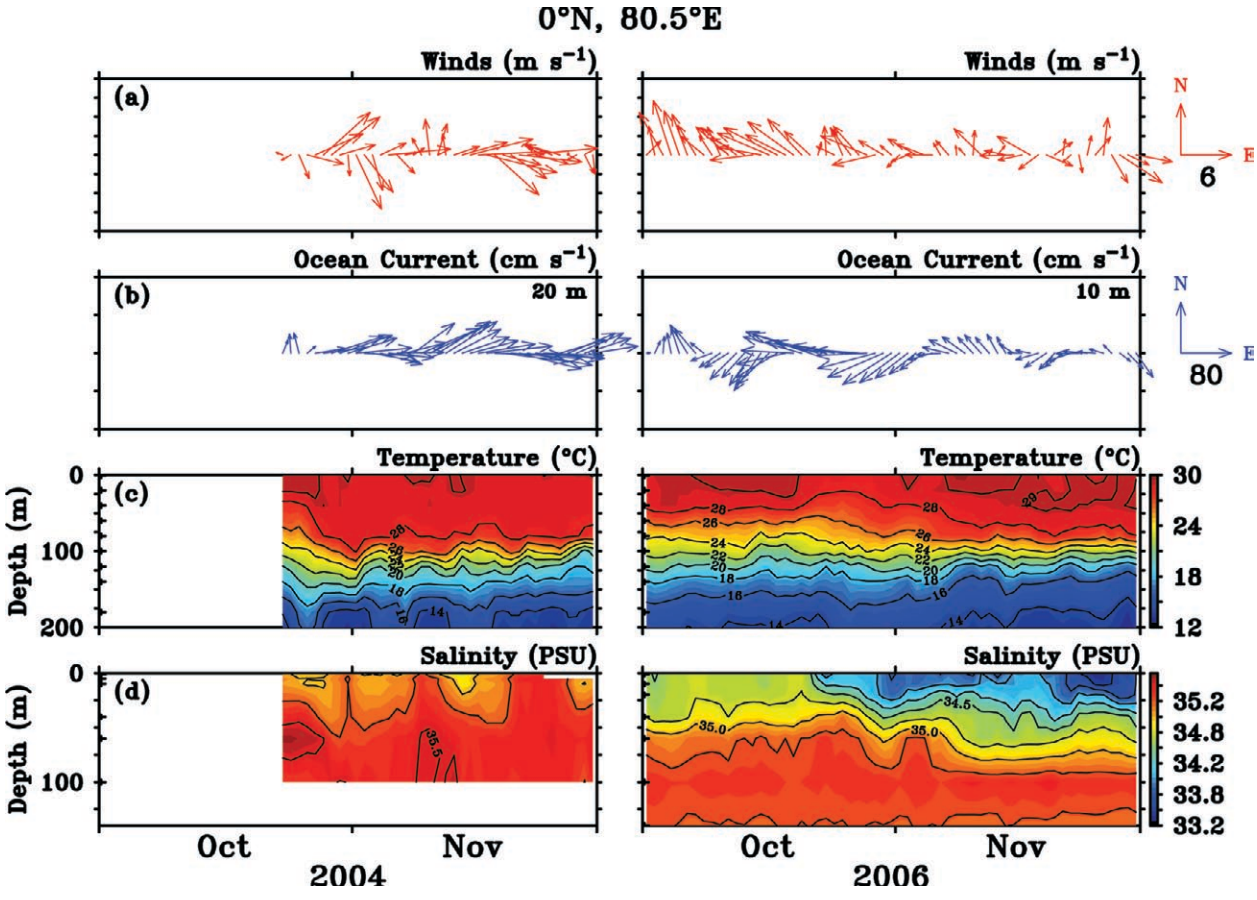

FIG. 8. Daily averaged data at 0°, 80.5°E for Oct–Nov 2004 (a neutral IOD year) and Oct–Nov 2006 (a positive IOD year, as illustrated in Fig. 2), with (a) wind vectors; (b) velocity vectors in the mixed layer (20-m depth in 2004 and 10-m depth in 2006); (c) temperature; and (d) salinity. Start of the time series in mid-Oct 2004 is coincident with the first deployment at this site.

currents. Finally, RAMA data will be valuable for quantitatively assessing the performance of oceanic and atmospheric dynamical models.

RAMA moorings, and in particular those specially instrumented reference sites for air–sea heat, moisture, and momentum fluxes, are a contribution to the Ocean Sustained Interdisciplinary Timeseries Environment Observation System (OceanSITES), a worldwide network of deep water stations providing high temporal resolution data for ocean research and environmental forecasting (www.oceansites.org/). In addition, RAMA is capable of accommodating biogeochemical sensors to support programs, such as the International Ocean Carbon Coordination Project (IOCCP; www.ioccp.org/) and the Sustained Indian Ocean Biogeochemical and Ecological Research (SIBER) program (Hood et al. 2008). RAMA will provide information on oceanic variability for the Joint Aerosol–Monsoon Experiment (JAMEX; Lau et al. 2008), which is a multinational study scheduled for November 2007–11 to investigate the effects of aerosols on ocean–atmosphere–land interactions that govern the Asian monsoon water cycle. In the wake of the December 2004 Asian tsunami, discussions are also underway with organizations involved in developing the Indian Ocean tsunami warning system on how best to coordinate implementation efforts with IndOOS. A joint RAMA and tsunami mooring cruise was conducted aboard the Indonesian Research Vessel *Baruna Jaya III* in September 2007 (www.noaanews.noaa.gov/stories2007/s2919.htm). In the longer term, it may beneficial to consider developing a multihazard moored buoy platform for both tsunami warnings and climate studies.

RAMA mooring stations provide convenient focal points around which to conduct short-term

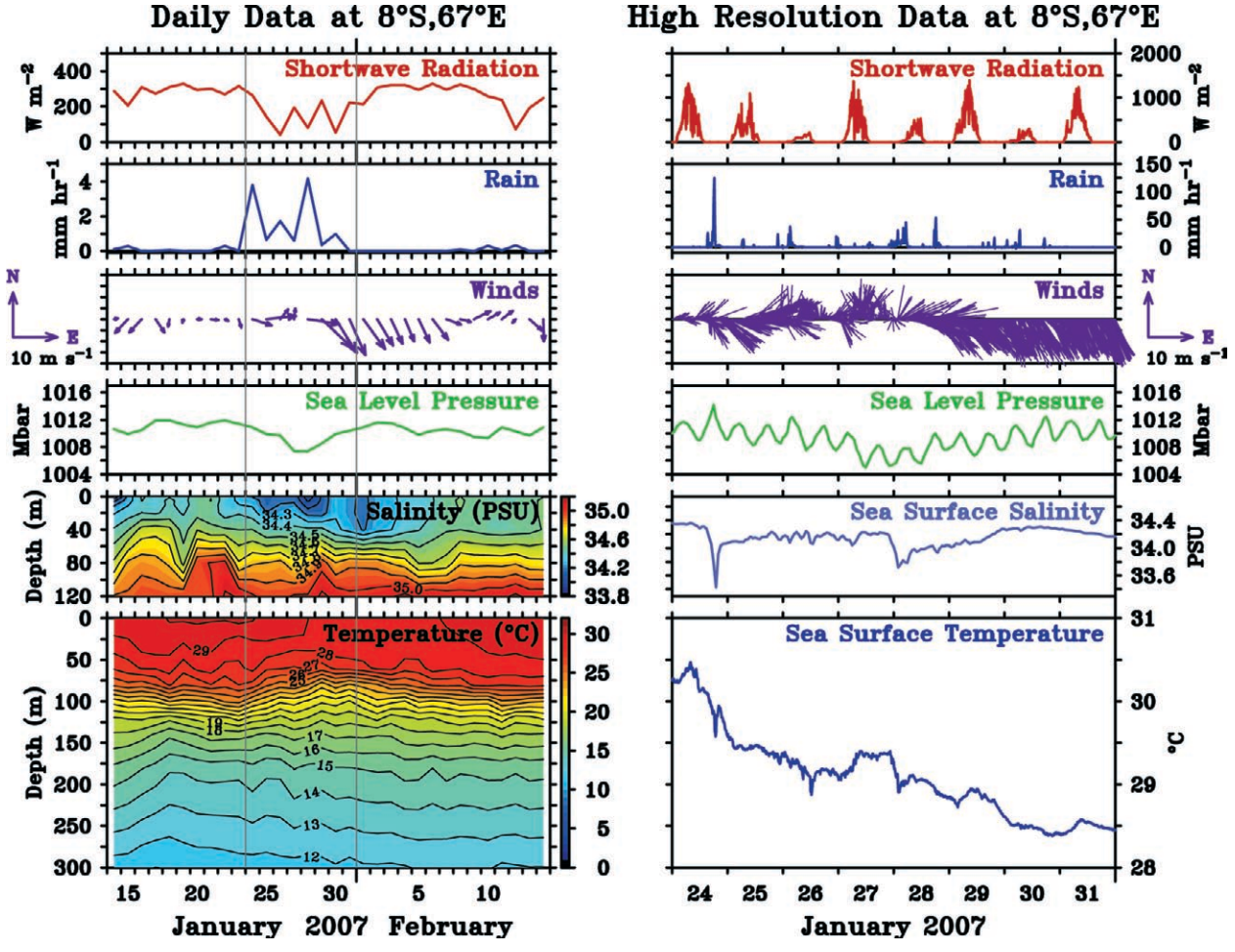

Fig. 9. Time series data from 8°S, 67°E in the Seychelles–Chagos thermocline ridge region during Jan–Feb 2007. (left) Daily averaged real-time data and (right) internally recorded 10-min data for selected variables during 24–31 Jan. The period highlighted on the right (delineated in the left panel by light gray lines) coincides with the passage nearby tropical cyclone Dora in the early stages of its development. (right) Arrow heads have been left off the vector winds for clarity.

process studies, such as MISMO, which took place in October–December 2006 centered at 0°, 80.5°E; and VASCO–Cirene, which took place in January–February 2007 near the mooring at 8°S, 67°E in the Seychelles–Chagos thermocline ridge region. These process studies benefited from RAMA, because they examined ocean–atmosphere interactions associated with the MJO for which high-resolution moored time series data are especially valuable (e.g., Vialard et al. 2008). RAMA, in turn, can benefit from process studies, since new knowledge gained from programs such as MISMO and VASCO–Cirene can feed back into design specifications for the moored array. Moreover, the VASCO–Cirene field campaign provided an opportunity to deploy the flux reference site mooring at 8°S, 67°E.

Neither RAMA nor IndOOS will address all the observational needs for understanding and predicting climate variability in the region, since we still lack a sustained in situ observing system for the atmosphere over the Indian Ocean. This lack of atmospheric data limits our understanding of convective processes, atmospheric circulation, and interactions of the atmosphere with the ocean. Regular cruises to service RAMA moorings can help mitigate this problem though by providing platforms of opportunity for routine meteorological observations.

In summary, full implementation of RAMA promises significant scientific and societal benefits. Challenges that we must overcome include securing the necessary resources to complete the array and forging long-lasting multinational partnerships to

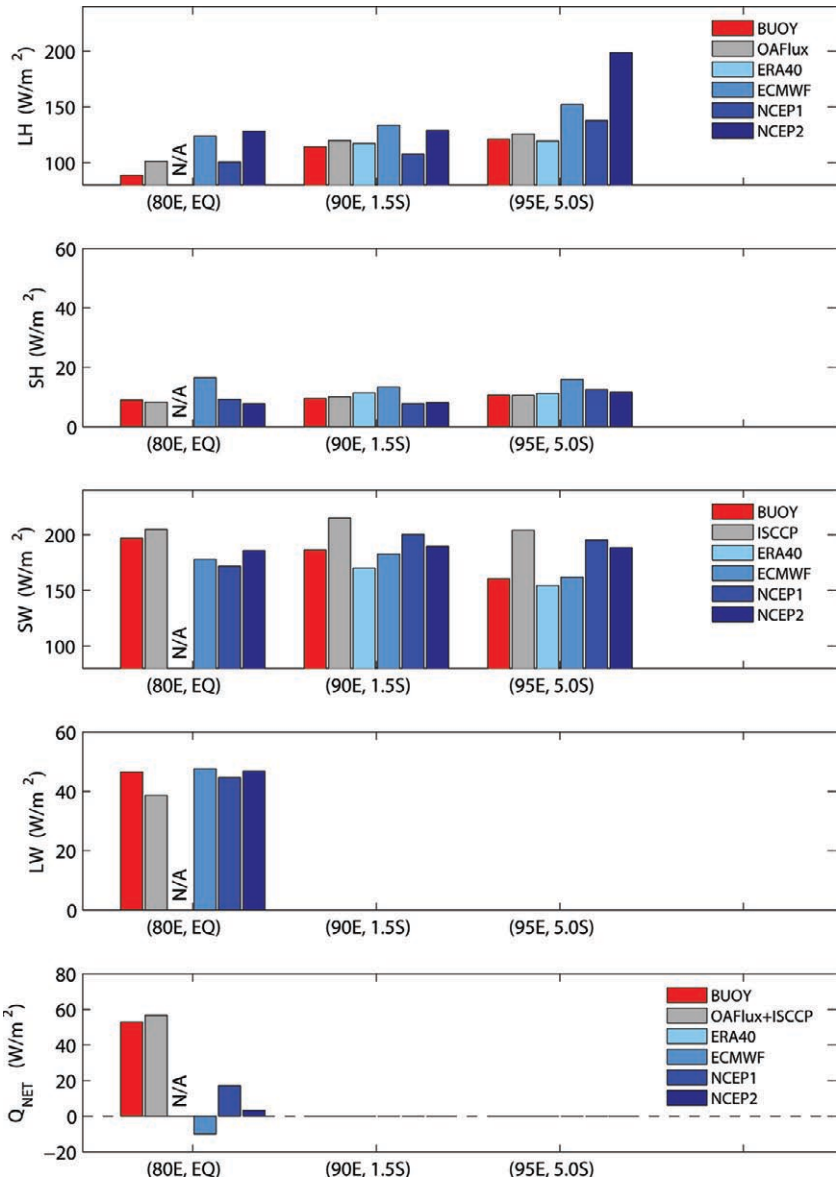

Fig. 10. Comparison of surface heat flux components at three RAMA sites with those computed from six different research and operational surface flux products: NCEP-1, NCEP-2, ECMWF, ERA-40, OA flux, and ISCCP (refer to Fig. 5). (top)–(bottom) Fluxes are latent heat flux (LH), sensible heat flux (SH), net shortwave radiation (SW), net longwave radiation (LW), and net surface heat flux (Q_{net}). Direct measurements of downwelling longwave radiation were made only at 0°, 80.5°E. Hence, LW and Q_{net} (which represents the sum of the four individual components) are shown only for this site. Turbulent fluxes were computed with the Coupled Ocean–Atmosphere Response Experiment (COARE) version 3.0 flux algorithm (Fairall et al. 2003) using daily averaged data. No warm-layer cool skin corrections were applied. Shortwave radiation was adjusted for 6% albedo. Upwelling longwave radiation at 0°, 80.5°E was computed assuming blackbody radiation from the sea surface, with an emissivity of 0.97. Comparisons were based on 70 days of overlapping data at 0°, 80.5°E between 23 Oct and 31 Dec 2004; 310 days at 1.5°S, 90°E between 23 Oct 2001 and 31 Aug 2002; and 287 days at 5°S, 95°E between 26 Oct 2001 and 31 Aug 2002.

sustain it. We know that success is possible though, because it has been achieved in the past for similar mooring programs of ambitious scope in the tropical Pacific and Atlantic.

ACKNOWLEDGMENTS. The authors would like to thank an anonymous reviewer, H. Annamalai, and *BAMS* subject matter editor Brian Mapes for helpful comments on an earlier version of this manuscript. We also acknowledge the International CLIVAR Project Office and the Intergovernmental Oceanographic Commission Perth regional office for supporting the Indian Ocean Panel. Many institutions and organizations have contributed to the implementation of RAMA and deserve mention: in India, the Ministry of Earth Sciences, the Indian National Center for Ocean Information Services, and the National Institute of Oceanography; in Japan, the Japan Agency for Marine–Earth Science and Technology, and the Ministry of Education, Sports, Culture, Science and Technology; in China, the State Oceanic Administration, First Institute of Oceanography, and the Ministry of Science and Technology; in Indonesia, the Agency for the Assessment and Application of Technology and the Agency for Marine and Fisheries Research; in France, the Institut Français de Recherche pour l'Exploitation de la Mer, the Institut de Recherche pour le Développement, and the Institut National des Sciences de l'Univers; in South Africa, the University of Capetown; in the United States, the NOAA Climate Program Office and the Office of Climate Observation; and the Agulhas and Somali Current Large Marine Ecosystems Project implemented by the United Nations Development Programme through funding from the Global Environment Facility. This manuscript was initiated while the first author was a guest at the University of Tasmania's Integrated Marine Observing System Office in Hobart, Australia. We dedicate this paper to the memory of our friend and colleague Fritz Schott, who inspired us through his scientific leadership, wise counsel, and deep understanding of the ocean.

REFERENCES

Alory, G., S. Wijffels, and G. Meyers, 2007: Observed temperature trends in the Indian Ocean over 1960–1999 and associated mechanisms. *Geophys. Res. Lett.,* **34,** L02606, doi:10.1029/2006GL028044.

Annamalai, H., and R. Murtugudde, 2004: Role of the Indian Ocean in regional climate variability. *Earth's Climate: The Ocean–Atmosphere Interaction, Geophys. Monogr.,* Vol. 147, Amer. Geophys. Union, 213–246.

——, H. Okajima, and M. Watanabe, 2007: Possible impact of the Indian Ocean SST on the Northern Hemisphere circulation during El Niño. *J. Climate,* **20,** 3164–3189.

Arguez, A., 2007: Supplement to State of the Climate in 2006. *Bull. Amer. Meteor. Soc.,* **88,** s1–s135.

Ashok, K., W.-L. Chan, T. Motoi, and T. Yamagata, 2004: Decadal variability of the Indian Ocean dipole. *Geophys. Res. Lett.,* **31,** L24207, doi:10.1029/2004GL021345.

Bessafi, M., and M. C. Wheeler, 2006: Modulation of south Indian Ocean tropical cyclones by the Madden–Julian oscillation and convectively coupled equatorial waves. *Mon. Wea. Rev.,* **134,** 638–656.

Bhat, G. S., and Coauthors, 2001: BOBMEX: The Bay of Bengal Monsoon Experiment. *Bull. Amer. Meteor. Soc.,* **82,** 2217–2243.

Bonjean, F., and G. E. S. Lagerloef, 2002: Diagnostic model and analysis of the surface currents in the tropical Pacific Ocean. *J. Phys. Oceanogr.,* **32,** 2938–2954.

Bourlès, B., and Coauthors, 2008: The PIRATA program: History, accomplishments, and future directions. *Bull. Amer. Meteor. Soc.,* **89,** 1111–1125.

Cane, M. A., and Coauthors, 1997: Twentieth-century sea surface temperature trends. *Science,* **275,** 957–960.

Chang, P., and Coauthors, 2006: Climate fluctuations of tropical coupled systems—The role of ocean dynamics. *J. Climate,* **19,** 5122–5174.

Cherchi, A., S. Gualdi, S. Behera, J. J. Luo, S. Masson, T. Yamagata, and A. Navarra, 2007: The influence of tropical Indian Ocean SST on the Indian summer monsoon. *J. Climate,* **20,** 3083–3105.

Clark, C. O., J. E. Cole, and P. J. Webster, 2000: Indian Ocean SST and Indian summer rainfall: Predictive relationships and their decadal variability. *J. Climate,* **13,** 2503–2519.

CLIVAR–GOOS Indian Ocean Panel and Coauthors, 2006: Understanding the role of the Indian Ocean in the climate system—Implementation plan for sustained observations. ICPO Publication Series 100, GOOS Rep. 152, 76 pp.

Cutler, A. N., and J. C. Swallow, 1984: Surface currents of the Indian Ocean (to 25°S, 100°E): Compiled from historical data archived by the meteorological office, Bracknell, U.K. Institute of Oceanographic Sciences Rep. 187, 8 pp.

de Ruijter, W. P. M., A. Biastoch, S. S. Drijfhout, J. R. E. Lutjeharms, R. P. Matano, T. Pichevin, P. J. van Leeuwen, and W. Weijer, 1999: Indian-Atlantic interocean exchange: Dynamics, estimation and impact. *J. Geophys. Res.,* **104** (C9), 20 885–20 910.

Duvel, J. P., and J. Vialard, 2007: Indo-Pacific sea surface temperature perturbations associated with intrasea-

sonal oscillations of tropical convection. *J. Climate,* **20,** 3056–3082.

——, C. Basdevant, H. Bellenger, G. Reverdin, A. Vargas, and J. Vialard, 2009: The aeroclipper: A new device to explore convective systems and cyclones. *Bull. Amer. Meteor. Soc.,* **90,** 63–71.

ECMWF, 1994: The description of the ECMWF/WCRP level III—A global atmospheric data archive. Tech. Attachment, 72 pp.

Fairall, C. F., E. F. Bradley, J. E. Hare, A. A. Grachev, and J. B. Edson, 2003: Bulk parameterization of air–sea fluxes: Updates and verification for the COARE algorithm. *J. Climate,* **16,** 571–591.

Feng, M., and G. Meyers, 2003: Interannual variability in the tropical Indian Ocean: A two-year time scale of IOD. *Deep-Sea Res. II,* **50,** 2263–2284.

——, ——, and S. Wijffels, 2001: Interannual Upper Ocean Variability in the Tropical Indian Ocean. *Geophys. Res. Lett.,* **28,** 4151–4154.

Fu, L.-L., 2007: Intraseasonal variability of the equatorial Indian Ocean observed from sea surface height, wind, and temperature data. *J. Phys. Oceanogr.,* **37,** 188–202.

Giannini, A., R. Saravanan, and P. Chang, 2003: Oceanic forcing of Sahel rainfall on interannual to interdecadal time scales. *Science,* **302,** 1027–1030.

Gordon, A. L., 2001: Interocean exchange. *Ocean Circulation and Climate,* G. Siedler, J. Church, and J. Gould, Eds., Academic Press, 303–314.

——, 2005: Oceanography of the Indonesian Seas and their Throughflow. *Oceanography,* **18,** 14–27.

Han, W., 2005: Origins and dynamics of the 90-day and 30–60-day variations in the equatorial Indian Ocean. *J. Phys. Oceanogr.,* **35,** 708–728.

——, P. Webster, R. Lukas, P. Hacker, and A. Hu, 2004: Impact of atmospheric intraseasonal variability in the Indian Ocean: Low-frequency rectification in equatorial surface current and transport. *J. Phys. Oceanogr.,* **34,** 1350–1372.

Harrison, D. E., and M. Carson, 2007: Is the world ocean warming? Upper-ocean temperature trends: 1950–2000. *J. Phys. Oceanogr.,* **37,** 174–187.

Hase, H., Y. Masumoto, Y. Kuroda, and K. Mizuno, 2008: Semiannual variability in temperature and salinity observed by Triangle Trans-Ocean Buoy Network (TRITON) buoys in the eastern tropical Indian Ocean. *J. Geophys. Res.,* **113,** C01016, doi:10.1029/2006JC004026.

Hermes, J. C., and C. J. C. Reason, 2008: Annual cycle of the South Indian Ocean (Seychelles-Chagos) thermocline ridge in a regional ocean model. *J. Geophys. Res.,* **113,** C04035, doi:10.1029/2007JC004363.

Higgins, R. W., and K. C. Mo, 1997: Persistent North Pacific circulation anomalies and the Tropical Intraseasonal Oscillation. *J. Climate,* **10,** 223–244.

Hoerling, M. P., and A. Kumar, 2003: The perfect ocean for drought. *Science,* **299,** 691–694.

——, J. W. Hurrell, and T. Xu, 2001: Tropical origins for recent North Atlantic climate change. *Science,* **292,** 90–92.

Hood, R. R., and Coauthors, 2008: Research opportunities and challenges in the Indian Ocean. *Eos, Trans. Amer. Geophys. Union,* **89,** doi:10.1029/2008GO130001.

Izumo, T., C. de Boyer Montégut, J.-J. Luo, S. K. Behera, S. Masson, and T. Yamagata, 2008: The role of the western Arabian Sea upwelling in Indian monsoon rainfall variability. *J. Climate,* **21,** 5603–5623.

Janowiak, J. E., and P. Xie, 1999: CAMS OPI: A global satellite–rain gauge merged product for real-time precipitation monitoring applications. *J. Climate,* **12,** 3335–3342.

Josey, S. A., E. C. Kent, and P. K. Taylor, 1999: New insights into the ocean heat budget closure problem from analysis of the SOC air–sea flux climatology. *J. Climate,* **12,** 2850–2880.

Kalnay, E., and Coauthors, 1996: The NCEP/NCAR 40-Year Reanalysis Project. *Bull. Amer. Meteor. Soc.,* **77,** 437–471.

Kanamitsu, M., W. Ebisuzaki, J. Woolen, J. Potter, S.-K. Yang, J. J. Hnilo, M. Fiorino, and G. L. Potter, 2002: NCEP–DEO AMIP-II Reanalysis (R-2). *Bull. Amer. Meteor. Soc.,* **83,** 1631–1643.

Knauss, J. A., 1961: The International Indian Ocean Expedition. *Science,* **134,** 1674–1676.

Knox, R. A., 1976: On a long series of measurements of Indian Ocean equatorial currents near Addu Atoll. *Deep-Sea Res.,* **23,** 211–222.

Krishna Kumar, K., B. Rajagopalan, M. A. Cane, 1999: On the weakening relationship between the Indian Monsoon and ENSO. *Science,* **284,** 2156–2159.

Krishnamurti, T., 1985: Summer Monsoon Experiment—A review. *Mon. Wea. Rev.,* **113,** 1590–1626.

Kuroda, Y., and Y. Amitani, 2000: TRITON: New ocean and atmospheric observing buoy network for monitoring ENSO. *Umi no Kenkyu,* **10,** 157–172.

Lau, K.-M., and Coauthors, 2008: The joint aerosol–monsoon experiment: A new challenge for monsoon climate research. *Bull. Amer. Meteor. Soc.,* **89,** 369–381.

Lee, T., and M. J. McPhaden, 2008: Decadal phase change in large-scale sea level and winds in the Indo-Pacific region at the end of the 20th century. *Geophys. Res. Lett.,* **35,** L01605, doi:10.1029/2007GL032419.

Levitus, S., J. Antonov, and T. Boyer, 2005: Warming of the world ocean, 1955–2003. *Geophys. Res. Lett.,* **32,** L02604, doi:10.1029/2004GL021592.

Liebmann, B., H. H. Hendon, and J. D. Glick, 1994: The

relationship between tropical cyclone of the western Pacific and Indian Oceans and the Madden–Julian oscillation. *J. Meteor. Soc. Japan,* **72,** 401–412.

Luo, J. J., S. Masson, S. Behera, and T. Yamagata, 2007: Experimental forecasts of the Indian Ocean dipole using a coupled OAGCM. *J. Climate,* **20,** 2178–2190.

Luyten, J. R., and D. H. Roemmich, 1982: Equatorial currents at semi-annual period in the Indian Ocean. *J. Phys. Oceanogr.,* **12,** 406–413.

——, M. Fieux, and J. Gonella, 1980: Equatorial currents in the western Indian Ocean. *Science,* **209,** 600–603.

Madden, R. A., and P. R. Julian, 1994: Observations of the 40–50-day tropical oscillation—A review. *Mon. Wea. Rev.,* **122,** 814–837.

Maloney, E. D., and D. L. Hartmann, 2000: Modulation of hurricane activity in the Gulf of Mexico by the Madden–Julian Oscillation. *Science,* **287,** 2002–2004.

Masumoto, Y., H. Hase, Y. Kuroda, H. Matsuura, and K. Takeuchi, 2005: Intraseasonal variability in the upper layer currents observed in the eastern equatorial Indian Ocean. *Geophys. Res. Lett.,* **32,** L02607, doi:10.1029/2004GL021896.

McPhaden, M. J., 1982: Variability in the central equatorial Indian Ocean, Part I: Ocean dynamics. *J. Mar. Res.,* **40,** 157–176.

——, 1999: Genesis and evolution of the 1997–98 El Niño. *Science,* **283,** 950–954.

——, and Coauthors, 1998: The Tropical Ocean-Global Atmosphere (TOGA) observing system: A decade of progress. *J. Geophys. Res.,* **103,** 14 169–14 240.

——, Y. Kuroda, and V. S. N. Murty, 2006a: Development of an Indian Ocean moored buoy array for climate studies. *CLIVAR Exchanges,* No. 11(4), International CLIVAR Project Office, Southampton, United Kingdom, 3–5.

——, X. Zhang, H. H. Hendon, and M. C. Wheeler, 2006b: Large scale dynamics and MJO forcing of ENSO variability. *Geophys. Res. Lett.,* **33,** L16702, doi:10.1029/2006GL026786.

Meyers, G., and R. Boscolo, 2006: The Indian Ocean Observing System (IndOOS). *CLIVAR Exchanges,* No. 11(4), International CLIVAR Project Office, Southampton, United Kingdom, 2–3.

——, P. McIntosh, L. Pigot, and M. Pook, 2007: The years of El Niño, La Niña, and interactions with the tropical Indian Ocean. *J. Climate,* **20,** 2872–2880.

Miura, H., M. Satoh, T. Nasuno, A. T. Noda, and K. Oouchi, 2007: A Madden–Julian Oscillation event realistically simulated by a global cloud-resolving model. *Science,* **318,** 1763–1765.

Murtugudde, R., J. P. McCreary, and A. J. Busalacchi, 2000: Oceanic processes associated with anomalous events in the Indian Ocean with relevance to 1997–1998. *J. Geophys. Res.,* **105,** 3295–3306.

Murty, V. S. N., and Coauthors, 2006: Indian Moorings: Deep-sea current meter moorings in the Eastern Equatorial Indian Ocean. *CLIVAR Exchanges,* No. 11(4), International CLIVAR Project Office, Southampton, United Kingdom, 5–8.

National Research Council, 1996: Learning to predict climate variations associated with El Niño and the Southern Oscillation: Accomplishments and legacies of the TOGA Program. National Academy Press, 171 pp.

——, 2000: Fifty years of ocean discovery: National Science Foundation 1950–2000. National Academy Press, 270 pp.

Oke, P. R., and A. Schiller, 2007: A model-based assessment and design of a tropical Indian Ocean mooring array. *J. Climate,* **20,** 3269–3283.

Reppin, J., F. Schott, J. Fishcher, and D. Quadfasel, 1999: Equatorial currents and transports in the upper central Indian Ocean. *J. Geophys. Res.,* **104,** 15 495–15 514.

Reynolds, R. W., N. A. Rayner, T. M. Smith, D. C. Stokes, and W. Q. Wang, 2002: An improved in situ and satellite SST analysis for climate. *J. Climate,* **15,** 1609–1625.

Ridderinkhof, H., and W. P. M. de Ruijter, 2003: Moored current observations in the Mozambique Channel. *Deep-Sea Res. II,* **50,** 1933–1955.

Rudnick, D. L., R. A. Weller, C. C. Eriksen, T. D. Dickey, J. Marra, and C. Langdon, 1997: Moored instruments weather Arabian Sea monsoons, yield data. *Eos, Trans. Amer. Geophys. Union,* **78,** 117, 120–121.

Saji, N. H., B. N. Goswami, P. N. Vinayachandran, and T. Yamagata, 1999: A dipole mode in the tropical Indian Ocean. *Nature,* **401,** 360–363.

Sanjeeva Rao, P., and D. R. Sikka, 2005: Intraseasonal variability of the summer monsoon over the North Indian Ocean as revealed by the BOBMEX and ARMEX field programs. *Pure Appl. Geophys.* **162,** 1481–1510.

Schott, F. A., and J. P. McCreary, 2001: The monsoon circulation of the Indian Ocean. *Prog. Oceanogr.,* **51,** 1–123.

——, ——, and G. C. Johnson, 2004: Shallow over-turning circulations of the tropical-subtropical oceans. *Earth Climate: The Ocean–Atmosphere Interaction, Geophys. Monogr.,* Vol. 147, Amer. Geophys. Union, 261–304.

——, S.-P. Xie, and J. P. McCreary Jr., 2009: Indian Ocean circulation and climate variability. *Rev. Geophys.,* **47,** RG1002, doi:10.1029/2007RG000245.

Seiki, A., and Y. N. Takayabu, 2007: Westerly wind bursts and their relationship with intraseasonal variations and ENSO. Part I: Statistics. *Mon. Wea. Rev.,* **135,** 3325–3345.

Sengupta, D., R. Senan, V. S. N. Murty, and V. Fernando, 2004: A biweekly mode in the equatorial Indian Ocean. *J. Geophys. Res.,* **109,** C10003, doi:10.1029/2004JC002329.

——, R. Senan, B. N. Goswami, and J. Vialard, 2007: Intraseasonal variability of equatorial Indian Ocean zonal currents. *J. Climate,* **20,** 3036–3055.

Shenoi, S. S. C., D. Shankar, and S. R. Shetye, 2002: Differences in heat budgets of the near-surface Arabian Sea and Bay of Bengal: Implications for the summer monsoon. *J. Geophys. Res.,* **107,** 3052, doi:10.1029/2000JC000679.

Shinoda, T., and W. Han, 2005: Influence of the Indian Ocean dipole on atmospheric subseasonal variability. *J. Climate,* **18,** 3891–3909.

Siedler, G., J. Church, and J. Gould, 2001: *Ocean Circulation and Climate: Observing and Modelling the Global Ocean*. International Geophysics Series, Vol. 77, Academic Press, 715 pp.

Slingo, J. M., and Coauthors, 1996: Intraseasonal oscillations in 15 atmospheric general circulation models: Results from an AMIP diagnostic subproject. *Climate Dyn.,* **12,** 325–357.

Smith, S. L., 2001: Understanding the Arabian Sea: Reflections on the 1994–1996 Arabian Sea Expedition. *Deep-Sea Res. II,* **48,** 1385–1402.

Syamsudin, F., A. Kaneko, and D. B. Haidvogel, 2004: Numerical and observational estimates of Indian Ocean Kelvin wave intrusion into Lombok Strait. *Geophys. Res. Lett.,* **31,** L24307, doi:10.1029/2004GL021227.

Taft, B. A., and J. A. Knauss, 1967: The equatorial undercurrent in the Indian Ocean as observed by the Lusiad Expedition. *Bull. Scripps Inst. Oceanogr.,* **9,** 163 pp.

Uppala, S. M., and Coauthors, 2005: The ERA-40 Re-Analysis. *Quart. J. Roy. Meteor. Soc.,* **131,** 2961–3012.

Vecchi, G. A., and D. E. Harrison, 2004: Interannual Indian rainfall variability and Indian Ocean sea surface temperature anomalies. *Earth Climate: The Ocean–Atmosphere Interaction, Geophys. Monogr.*, Vol. 147, Amer. Geophys. Union, 247–260.

——, and M. J. Harrison, 2007: An observing system simulation experiment for the Indian Ocean. *J. Climate,* **20,** 3300–3319.

Vialard, J., G. Foltz, M. McPhaden, J. P. Duvel, and C. de Boyer Montégut, 2008: Strong Indian Ocean cooling driven by the Madden-Julian oscillation in late 2007 and early 2008. *Geophys. Res. Lett.,* **35,** L19608, doi:10.1029/2008GL035238.

——, and Coauthors, 2009: Cirene: Air–sea interactions in the Seychelles–Chagos thermocline ridge region. *Bull. Amer. Meteor. Soc.,* **90,** 45–61.

Wainwright, L., G. Meyers, S. Wijffels, and L. Pigot, 2008: Change in the Indonesian Throughflow with the climate shift of 1976/77. *Geophys. Res. Lett.,* **35,** L03604, doi:10.1029/2007GL031911.

Wajsowicz, R. C., 2005: Potential predictability of tropical Indian Ocean SST anomalies. *Geophys. Res. Lett.,* **32,** L24702, doi:10.1029/2005GL024169.

Waliser, D. E., K.-M. Lau, and J.-H. Kim, 1999: The influence of coupled sea surface temperatures on the Madden–Julian oscillation: A model perturbation experiment. *J. Atmos. Sci.,* **56,** 333–358.

Waple, A. M., and J. H. Lawrimore, 2003: State of the Climate in 2002. *Bull. Amer. Meteor. Soc.,* **84,** 800.

Webster, P. J., and C. Hoyos, 2004: Prediction of monsoon rainfall and river discharge on 15–30-day time scales. *Bull. Amer. Meteor. Soc.,* **85,** 1745–1765.

——, and Coauthors, 2002: The JASMINE pilot study. *Bull. Amer. Meteor. Soc.,* **83,** 1603–1630.

Webster, P. W., A. M. Moore, J. P. Loschnigg, and R. R. Lebben, 1999: Coupled ocean-atmosphere dynamics in the Indian Ocean during 1997-98. *Nature,* **401,** 356–360.

Wijffels, S., and G. Meyers, 2004: An intersection of oceanic waveguides: Variability in the Indonesian throughflow region. *J. Phys. Oceanogr.,* **34,** 1232–1253.

Woolnough, S. J., F. Vitart, and M. Balmaseda, 2007: The role of the ocean in the Madden-Julian Oscillation: Sensitivity of an MJO forecast to ocean coupling. *Quart. J. Roy. Meteor. Soc.,* **133,** 117–128.

Wyrtki, K., 1973: An equatorial jet in the Indian Ocean. *Science,* **181,** 262–264.

Xie, S.-P., H. Annamalai, F. A. Schott, and J. P. McCreary, 2002: Structure and mechanisms of South Indian Ocean climate variability. *J. Climate,* **15,** 864–878.

Yamagata, T., S. K. Behera, J.-J. Luo, S. Masson, M. Jury, and S. A. Rao, 2004: Coupled ocean–atmosphere variability in the tropical Indian Ocean. *Earth Climate: The Ocean-Atmosphere Interaction, Geophys. Monogr.,* No. 147, AGU, 189–212.

Yang, J., Q. Liu, S.-P. Xie, Z. Liu, and L. Wu, 2007: Impact of the Indian Ocean SST basin mode on the Asian summer monsoon. *Geophys. Res. Lett.,* **34,** L02708, doi:10.1029/2006GL028571.

Yaremchuk, M., 2006: Sea surface salinity constrains rainfall estimates over tropical oceans. *Geophys. Res. Lett.,* **33,** L15605, doi:10.1029/2006GL026582.

Yokoi, T., T. Tozuka, and T. Yamagata, 2008: Seasonal variation of the Seychelles Dome. *J. Climate,* **21,** 3740–3754.

Yoneyama, K., and Coauthors, 2008: MISMO field experiment in the equatorial Indian Ocean. *Bull. Amer. Meteor. Soc.,* **89,** 1889–1903.

Yu, L., and R. A. Weller, 2007: Objectively analyzed air–sea heat fluxes for the global ice-free oceans (1981–2005). *Bull. Amer. Meteor. Soc.,* **88,** 527–539.

——, X. Jin, and R. A. Weller, 2007: Annual, seasonal, and interannual variability of air–sea heat fluxes in the Indian Ocean. *J. Climate,* **20,** 3190–3209.

Yu, W., B. Xiang, L. Liu, and N. Liu, 2005: Understanding the origins of interannual thermocline variations in the tropical Indian Ocean. *Geophys. Res. Lett.,* **32,** L24706, doi:10.1029/2005GL024327.

Yu, Z., and J. P. McCreary Jr., 2004: Assessing precipitation products in the Indian Ocean using an ocean model. *J. Geophys. Res.,* **109,** C05013, doi:10.1029/2003JC002106.

Zhang, C., 2005: Madden-Julian Oscillation. *Rev. Geophys.,* **43,** RG2003, doi:10.1029/2004RG000158.

Zhang, Y., W. B. Rossow, A. A. Lacis, V. Oinas, and M. I. Mishchenko, 2004: Calculation of radiative fluxes from the surface to top of atmosphere based on ISCCP and other global data sets: Refinements of the radiative transfer model and the input data. *J. Geophys. Res.,* **109,** D19105, doi:10.1029/2003JD004457.